Journal of Renewable Materials

Tech Science Press

DOI: 10.32604/jrm.2024.052172

ARTICLE

Thermo-Mechanical, Physico-Chemical, Morphological, and Fire Characteristics of Eco-Friendly Particleboard Manufactured with Phosphorylated Lignin Addition

Apri Heri Iswanto[1,*], Harisyah Manurung[1], Asma Sohail[2], Lee Seng Hua[3,9], Petar Antov[4], Deded Sarip Nawawi[5], Sarah Latifah[5], Dewi Shafa Kayla[5,6], Sukma Surya Kusumah[6], Muhammad Adly Rahandi Lubis[6], Linda Makovická Osvaldová[7], Mohd. Hazwan Hussin[8], Rangabhashiyam Selvasembian[9], Lum Wei Chen[10], Puji Rahmawati Nurcahyani[6], Nam Hun Kim[11] and Widya Fatriasari[6]

[1]Department of Forest Products, Faculty of Forestry, Universitas Sumatera Utara, Kampus USU Padang Bulan, Medan, North Sumatra, 20155, Indonesia

[2]Department of Chemistry, Lahore College for Women University, Lahore, 4444, Pakistan

[3]Department of Wood Industry, Faculty of Applied Sciences, Universiti Teknologi MARA (UiTM), Cawangan Pahang Kampus Jengka, Shah Alam, 26400, Malaysia

[4]Faculty of Forest Industry, University of Forestry, Sofia, 1797, Bulgaria

[5]Department of Forest Product, Faculty of Forestry and Environment, IPB University, Bogor, 16680, Indonesia

[6]Research Center for Biomass and Bioproducts, National Research and Innovation Agency (BRIN), Cibinong, 16911, Indonesia

[7]Department of Forest Engineering, Faculty of Security Engineering, University of Zilina, Zilina, 01001, Slovakia

[8]Materials Technology Research Group (MaTReC), School of Chemical Sciences, Universiti Sains Malaysia, Minden, Penang, 11800, Malaysia

[9]Department of Environmental Science and Engineering, School of Engineering and Sciences, SRM University-AP, Amaravati, Andhra Pradesh, 522240, India

[10]Department of Bio and Natural Resources, Faculty of Bioengineering and Technology, Universiti Malaysia Kelantan, Jeli, Kelantan, 17600, Malaysia

[11]Department of Forest Biomaterials Engineering, College of Forest and Environmental Sciences, Kangwon National University, Chuncheon, 24341, Republic of Korea

[*]Corresponding Author: Apri Heri Iswanto. Email: apri@usu.ac.id

Received: 25 March 2024 Accepted: 28 June 2024 Published: 21 August 2024

ABSTRACT

Lignin, lignosulfonate, and synthesized phosphorylated lignosulfonate were introduced as green fillers in citric acid-sucrose adhesives for bonding particleboard fabricated from areca leaf sheath (ALS). The characteristics of particleboards were compared to that of ultralow emitting formaldehyde (ULEF-UF). The fillers derived from *Eucalyptus spp*. kraft-lignin were added for flame retardancy enhancement. 10% of each lignin and modified lignin was added into the ULEF-UF and citric acid-sucrose bonded particleboards. Analyses applied to particleboards included thermal characteristics, X-ray diffraction analysis (XRD), morphological properties, Fourier transform infrared spectroscopy (FTIR), as well as physical, mechanical, and fire resistance characteristics of the laboratory-fabricated particleboards. Lignin and modified lignin resulted in improved thermal stability of the composites bonded with ULEF-UF while the improvement in the particleboard bonded with citric acid-sucrose was not significant. The introduction of filler exerted a higher influence on the UF-bonded particleboards

compared to composites fabricated with citric acid-sucrose. Generally, the presence of lignin, lignosulfonate, and phosphorylated lignosulfonate enhanced the mechanical strength of the ULEF-bonded particleboards, although their dimensional stability has deteriorated. Markedly, the use of lignin and lignosulfonate enhanced the fire resistance of the particleboards produced with lower observed weight loss. All laboratory particleboards exhibited satisfactory fire resistance, attaining a V-0 rating in according to the UL-94 standard.

KEYWORDS

Modified lignin; eco-friendly particleboard; fire and thermal properties; citric acid-sucrose; ultralow-emitting urea-formaldehyde resin

1 Introduction

In recent years, the global demand for and manufacturing of wood-based panels, including particleboard panels, has increased substantially. According to the Imarcgroup [1], in 2023, the worldwide particleboard market was estimated to $23 billion, and it is forecasted to increase to $31.3 billion by 2032, with a compound annual growth rate (CAGR) of 3.4% projected from 2024 to 2032. Increasing environmental awareness and the desire for environmentally friendly wood-based products that are free from hazardous Volatile Organic Compounds (VOCs) such as formaldehyde have stimulated advances in the use of particleboard bonded with novel urea-formaldehyde (UF) adhesives. These adhesives are characterized by significantly low or minimal formaldehyde emissions, indicated by low formaldehyde-to-urea molar ratios with formaldehyde-to-urea ratios ranging from 2.0 to 4.0 [2,3]. The resulting material was termed ultralow-emitting formaldehyde urea-formaldehyde (ULEF-UF) resin with a formaldehyde/urea ratio of 0.8. The wood-based composites bonded with these UF resins can achieve the super E0 emission level, whereas those bonded with regular UF resin are typically classified as E0 or E1 [4].

The incorporation of different types of formaldehyde scavengers, including synthetic, natural (biobased), and nano scavenger materials, into standard synthetic wood adhesives can reduce harmful free formaldehyde emissions from wood-based panels [5,6], the surface coating of wood composites, and the use of formaldehyde-free wood adhesives such as polymethylene diphenyl diisocyanate (pMDI) or natural biobased adhesive formulations [7,8].

Various types of natural nonformaldehyde adhesives, such as sucrose [9], citric acid [10], and a combination of citric acid and sucrose [11], are receiving increasing amounts of attention. Citric acid solution is supplemented with sucrose to enhance bond performance [9,12]. For composite products with three carboxyl groups that can attach esters to hydroxyl groups in wood, citric acid is a possible binding agent. When sugar is added, hydroxyl groups are produced, and the quantity of ester groups increases [13]. Other natural adhesives for wood derivative applications include lignin (condensed and hydrolyzed), tannins, soybeans, starch (corn) [14], carboxylic acid, vegetable oil, natural rubber, carbohydrates, protein and plant extracts [14,15]. In terms of commercial utilization, tannin bioadhesives have advanced on the market, with some formulations being developed for large-scale industrial manufacturing [16,17].

A promising strategy to support the forest-based sector's transition toward a circular bioeconomy is to capitalize on the industrial benefits of substitute materials, such as recycled wood waste, as well as agricultural biomass, in particleboard manufacturing. This is driven by the heightened global demand for wood and wood-based products [18,19].

Areca leaf sheaths (ALS) are a byproduct of areca palm (*Areca catechu L.*) plantations. According to the data reported by the Geospatial Information Agency and Director General of Plantations, Ministry of

Agriculture of Indonesia, the area of areca nut plantations in 2020 was approximately 147,890 hectares. ALS is a hard waste material with good tensile strength [20] and can be utilized for reinforcing fibers [21]. Despite its potential, the use of ALS is still limited, mainly for packaging materials [22] and composite boards to substitute synthetic fibers combined with nonenvironmentally friendly [23]. Madyaratri et al. reported the development of eco-friendly particleboard from ALS that exhibited satisfactory mechanical and physical properties and improved fire resistance by using ULEF-UF resin and biobased additives (lignosulfonate and kraft lignin) [24].

Lignin is present as a constituent of wood, and its level fluctuates depending on the wood species. Additionally, lignin naturally contains a diverse array of aromatic compounds. In recent years, lignin valorization has become an issue of great importance due to the enhanced utilization of wood components in numerous value-added applications in line with the requirements of the circular bioeconomy [25]. On the other hand, the growth of the pulp industry tends to increase with the global production of paperboard and paper, reaching ±414 million metric tons in 2022 [26]. These industries produce black liquor, which contains lignin, as a byproduct. In Indonesia, *Eucalyptus spp*. is a hardwood species extensively utilized as a primary material in the pulp and paper industry. In previous reports, Eucalyptus lignin subjected to 3 washing cycles of HCl precipitation had a relatively high purity of 85.88% and a yield of 39.28%. Lignosulfonate synthesis from this lignin afforded 93.39% yield and 71.89% purity [27].

Lignin can be incorporated with polymers or as a fire-retardant (FR) additive in composite systems [28,29]. In woody or nonwoody composites, lignin can be mixed with adhesives to improve the fire retardancy performance. Phenolic lignin can suppress flames, but the degree of fire behavior varies depending on the lignin extraction process and its origin. Additionally, lignin has good thermal stability, reduces degradation during combustion, and increases the char (carbonizing substance) residue. Char can act as a shield on the polymer surface, which inhibits the entry of oxygen into the polymer [30–32]. It is possible to alter the lignin structure to produce lignin FR with strong FR endurance and efficiency [33]. Usually, chemicals such as phosphorus, nitrogen, and metal components are added to the reaction [34]. Lignin can also be functionalized to increase its resistance to fire by using phosphorus-based materials (lignin phosphorylation) [35]. Phosphorus can inhibit flames in both the gas and condensed phases by interacting with the polymer matrix and initiating char production. Phosphorus can increase the amount of carbon residue, which remains more stable at high temperatures, by promoting dehydration and decarboxylation. The flammability properties of phosphorylated lignin are also reduced. Isolated lignin has low solubility in water in the acidic pH and neutral [36]; thus, modification through the sulfonation process is needed for lignosulfonate and lignosulfonate phosphorus to facilitate its application as an FR, which is expected to improve fire resistance properties.

The innovation of wood-based composite materials has garnered significant attention from researchers due to the shift from a linear to a cyclical bioeconomy model in the wood-based panel sector. Additionally, targets of low-carbon bioeconomy modes are expected to increase environmental awareness regarding the use of unsustainable oil-based fuels. Moreover, current legislative requirements emphasize the importance of formaldehyde-free emissions from wood-based composites [37]. Therefore, the use of ULEF-UF resins and citric acid-sucrose adhesives for bonding wood composites represents a viable solution to achieve these goals.

However, the manufactured biocomposites are characterized by several drawbacks, such as flammability. The incorporation of FR compounds, e.g., phosphorylated lignin, as fillers into biocomposites represents a promising solution to enhance their flame retardancy [38]. For the first time, lignin, lignosulfonate, and synthesized phosphorylated lignosulfonate were introduced as green fillers of

citric acid-sucrose adhesives in particleboard fabricated from areca leaf sheath (ALS). These characteristics of the particleboard samples were compared to those of ULEF-UF.

Previous research has demonstrated the efficacy of lignin and lignosulfonate in improving the flame retardancy of impregnated rattan [27]. Madyaratri et al. also noted the development of eco-friendly particleboard, which exhibited satisfactory physical and mechanical properties and increased fire resistance, by using ULEF-UF resin and biobased additives (lignosulfonate and kraft lignin) [24]. The research objective was to prepare and assess the properties of particleboard joined with citric acid-sucrose and ULEF-UF adhesives incorporating both lignin and modified lignin for enhanced performance.

2 Materials and Methods

2.1 Material Preparation

The components employed in this investigation included *Eucalyptus spp*. kraft-lignin, which was derived from black liquor sourced from PT Toba Pulp Lestari, which is located in North Sumatra, Indonesia, and 14 mesh areca leaf sheath particles. Additionally, HCl (Merck, Darmstadt, Germany), distilled water (Bratachem, Bandung, Indonesia), $Na_2S_2O_5$ (Merck, Darmstadt, Germany), 10% NaOH (Merck, Darmstadt, Germany), areca leaf sheath particles of 14 mesh (PT Greenei Alam Indonesia, PT GAI, Tangerang, Indonesia), anhydrous technical citric acid (Weifang Ensign Industry Co., Ltd., Weifang, China), sucrose (Gulaku, Lampung, Indonesia), and $POCl_3$ (Central Drug House (P) Ltd., New Delhi, India) were utilized. The procedure for isolating lignin and producing lignosulfonate followed the methodology outlined by Madyaratri et al. [27], with comprehensive elaboration provided in Sections 2.2.1 and 2.2.2.

2.2 Preparation of Filler for Particleboard

2.2.1 Lignin Isolation

This lignin isolation process refers to previous research conducted by Madyaratri et al. [27]. This research utilized 50 g of black liquor from Eucalyptus biomass. The black liquor was diluted with distilled water (DI) water at a ratio of 1:10. Subsequently, 2 M HCl was added dropwise while stirring until the pH reached 2. The sample solution was stored at room temperature (25°C) for 24 h to ensure complete sedimentation. Following sedimentation, the solution was drained by removing the top (solution) using pipetting, followed by successive washing with 350 mL of reverse osmosis (RO) water for each washing cycle; this process was repeated up to 3 times. The precipitate obtained was subsequently filtered and placed onto a tray covered with heat-resistant plastic, followed by heating in an oven at 45°C for 24 h. Through this isolation procedure, the yield and purity (acid-soluble lignin, ASL, and acid-insoluble lignin, AIL) of lignin were 39.28% and 85.88%, respectively, with a water content of 1.58%, ash content of 4.20% and total ph-OH content of 6.74% [27].

2.2.2 Lignosulfonate Synthesis

The lignosulfonate synthesis process was carried out according to previous research conducted by Madyaratri et al. [27]. Approximately 5 g of *Eucalyptus spp*. lignin was washed three times, and 2.5 g of sodium metabisulfite ($Na_2S_2O_5$) was mixed with 150 ml of DI water. The solution was added to 10% NaOH until a pH of 7 was reached. The synthesis process was conducted in a three-neck flask with stirring for 4 h at 90°C, followed by placing the solution in a water bath at 85°C for concentration purposes. The concentrated solution was filtered using a Buchner funnel to separate the remaining unreacted lignin. The filtrate was heated in an oven at 60°C overnight for drying. The dried lignosulfonate was pulverized. From the synthesis, the purity and yield obtained were 71.89 % and 93.39%, respectively [27].

2.2.3 Phosphorus Lignosulfonate Synthesis

The phosphorus lignosulfonate synthesis process was performed according to a previous study conducted by Costes et al. [39] with modifications. Five grams of lignosulfonate was placed in a three-necked flask and mixed with 50 mL of water while stirring and heating to 40°C. Then, 2 mL of $PoCl_3$ was gradually added to the solution. The synthesis was then conducted for 7 h at 50°C. Subsequently, the liquid was strained using filter paper and a glass funnel. The synthesized phosphorous lignosulfonate was placed in Petri dishes coated with heat-resistant plastic and then dried in a vacuum oven (500 mbar) at 60°C for 24 h.

2.3 Synthesis of Low-Emitting Urea Formaldehyde (ULEF-UF)

A ULEF-UF resin was prepared with a formaldehyde/urea molar ratio of 0.8 (Indonesian registered patent number P00202106099). Initially, formaldehyde was heated to 40°C in a beaker while maintaining a pH of 8.0, and the solution was stirred at 300–350 rpm using a digital stirrer. If the pH of the solution remained low, NaOH solution was gently added. After 1 h of stirring, the temperature of the mixture was increased to 90°C. Subsequently, the first portion of urea was incrementally added while ensuring that the pH remained at 8.0. After one-hour, formic acid was gradually added to the mixture to adjust the pH to between 4.5 and 5.0. Next, the second portion of urea was added and stirred for an additional 30 min until the solution's pH reached 4.6, after a total reaction time of 2.5 h at 80°C. The properties of ULEF-EF (Table 1) were determined and reported in our parallel study [40].

Table 1: Basic properties of ultralow-emission urea formaldehyde adhesive

Characteristics of adhesives	Adhesive types	
	ULEF-UF*	UF (SNI 06-0060-1987)
Color	Milky white	Milky white
pH (25°C)	8.07	7.6–8.6
Gelation Time (min)	4.75 ± 1.48	<60
Viscosity (mPa·s)	152.9	100–150

Note: Remarks: Adapted with permission from reference [40]. License number: 5806960187757. Copyright ©2024, Elsevier.

2.4 Physico-Chemical Properties of Modified ULEF-UF and Citric Acid-Sucrose Adhesives

The physico-chemical properties of the modified ULEF-UF and citric acid-sucrose adhesives incorporated with lignin, lignosulfonate, and lignosulfonate phosphorus at a 0.8 F/U molar ratio, such as the gelation time, density, solid content, pH, cohesion strength, and viscosity, were determined according to published work [41]. The gelation time of the adhesive was calculated using a gelation timer (Techne GT-6, Coleparmer, Vernon Hills, IL, USA) by placing the adhesive sample in a glass tube. The gel time meter was positioned so that the needle was submerged in the sample. The adhesive gelatinization time was measured at 25°C. Adhesive gelation timeout occurs when the timer stops automatically [42]. The adhesive viscosity was measured using a rotational rheometer (RheOLaB QC, Anton Paar, Graz, Austria) with concentric cylinder (CC) type spindle no. 27 at 25°C and a dynamic shear rate of 1–100 s^{-1} for 120 s. The density of the adhesives with filler was determined via the gravimetry method using a 25 mL pycnometer carefully filled with the adhesive. The mass of the filled pycnometer was then determined. The density is calculated by dividing the mass of the sample by the volume of the pycnometer. The solid content of the adhesives with filler was also determined by using the gravimetry method. The petri dishes were oven-dried at 105°C for 4 h. The cup was then placed in a desiccator for 30 min, and the weight was recorded. A Petri dish containing 1 g of sample was weighed. The sample was oven-dried at 105°C

for 3 h and then kept in a desiccator for 30 min before being weighed. The solid content of the adhesive was calculated using the formula reported by Renzy Hariz et al. [42].

2.5 Particleboard Production

The particleboard samples were fabricated under laboratory conditions employing various types of fillers as fire retardants and different adhesive systems, as detailed in Table 2. The fire retardants utilized included lignin (L), lignosulfonate (LS), and phosphorylated lignosulfonate (PLS). The adhesive systems tested comprised citric acid-sucrose adhesives and ULEF-UF resin. Approximately 10% of the filler (lignin and phosphorylated lignosulfonate) was dissolved in a 10% NaOH solution, while lignosulfonate was dissolved in water at a 10% concentration before being mixed with citric acid-sucrose adhesive (1:9) at a concentration of 59%, with an adhesive content of 20 wt.% of the dry mass of the particles. The ULEF-UF adhesive with a 15% particle dry mass (Indonesian registered patent P00202104450) was also mixed with the particles and 10% filler. Following the methodology outlined in previous research [24], particleboards were manufactured with dimensions of 250 mm in length, 250 mm in width, and 10 mm in thickness, targeting a density of 0.8 g/cm³. To ensure a uniform mixture, the adhesive solution and areca powder were combined using a drum mixer equipped with a compressor and spray cannon. The mixtures were then molded to size and subjected to hot pressing at temperatures of 200°C (for citric acid-sucrose adhesives) and 150°C (for ULEF-UF) for 10 min at a specific pressure of 2.7 MPa. The laboratory-fabricated particleboard samples were stored at 20°C ± 2°C and a relative humidity of 65% for 1 week. They were then cut to standardized sizes for evaluation of physical properties, mechanical properties, and fire resistance tests.

Table 2: Particleboard treatments with lignin/lignosulfonate/phosphorylated lignosulfonate as the FR filler

Particleboard	Sample codes	wt.% of FR in 100% composites
Particleboard with UF adhesives (without flame retardant)	PKUF	0
Particleboard with UF adhesives/lignin	PUFL	10
Particleboard with UF adhesives/lignosulfonate	PUFLs	10
Particleboard with UF adhesives/phosphorylated lignosulfonate	PUFLsP	10
Particleboard with citric acid-sucrose adhesives (without flame retardant)	PASK	0
Particleboard with citric acid-sucrose adhesives/lignin	PASL	10
Particleboard with citric acid-sucrose adhesives/lignosulfonate	PASLs	10
Particleboard with citric acid-sucrose adhesives/phosphorylated lignosulfonate	PASLsP	10

2.6 Characterization of the Particleboard

2.6.1 Thermal Properties by Thermal Gravimetry Analysis (TGA)

Approximately 12–20 mg of each particleboard sample was weighed into a standard ceramic crucible in a thermogravimetric analyzer (LABSYS evo, Setaram Instrumentation, Caluire, France). The temperature was then increased at a rate of 10°C per min until it reached 800°C. The analysis was conducted in a nitrogen atmosphere by adding nitrogen gas at a flow rate of 50 mL/min. Calisto processing software was used to construct a weight loss curve at a certain temperature according to the TGA results.

2.6.2 FTIR Analysis

FTIR or Fourier transform infrared spectroscopy was employed to investigate the functional groups of both the filler and nonfiller particleboard. The method used was universal attenuated total reflectance (UATR) (Bruker type alpha, Bruker GmbH, Mannheim, Germany). By using FTIR, the functional groups of lignin were examined. At wavelengths ranging from 400 to 4000 cm, the analysis was captured with an average of 16 scan resolutions of 4 cm^{-1}.

2.6.3 XRD Analysis

XRD analysis of the particleboard was accomplished by converting the particleboard into powder, which was then placed in the glass sample before being input into the glass sample holder in an XRD machine (Miniflex type, Rigaku, Tokyo, Japan). The 2ø angle was 0°–80° with a tube current of 15 mA and a tube voltage of 30 kV. The crystallinity of the samples was determined by using Origin Pro software to determine the amorphous area and the crystalline area with Lorentz fitting. This equation is used for calculations based on Eq. (1).

$$\text{Degree of crystallinity } (\%) = \frac{crystalline\ area}{crystalline\ area + amorhous\ area} \times 100 \quad (1)$$

2.6.4 Mechanical and Physical Properties

The physical and mechanical characteristics were determined based on JIS A 5908-2003 [43]. The laboratory-made particleboard was tested for material density, water absorption capacity, moisture content, and thickness swelling underwater, as well as for its mechanical properties, including modulus of rupture (MOR), modulus of elasticity (MOE) with testing dimensions of 200 mm × 50 mm × 10 mm, life span of 150 mm, crosshead speed of 10 mm/min and internal bond strength (IB) with dimensions of 50 cm × 50 cm × 10 mm and a crosshead speed of 2 mm/min. The density of the particleboard samples with dimensions of 100 mm × 100 mm × 10 mm was determined using Eq. (2). These strengths were tested by a UTM (Universal Testing Machine AGS-X 50 kN, Shimadzu, Kyoto, Japan). The dry samples were weighed to determine their mass, and the volume was determined by measuring the dimensions, including thickness, length, and width, using a digital caliper.

$$\text{Density } \left(g/cm^3\right) = \frac{sample\ weight\ (g)}{sample\ volume\ (m^3)} \quad (2)$$

The moisture content (MC) of the particleboard was determined by drying it for 24 h at a temperature of 103°C ± 2°C. After cooling in a desiccator, the samples were weighed to obtain their final weight using an analytical balance. Eq. (3) was utilized in the moisture content calculation.

$$\text{Moisture content } (\%) = \frac{the\ initial\ weight\ of\ the\ sample - oven\ dry\ weight\ of\ the\ sample}{oven\ dry\ weight\ of\ the\ sample} \times 100\% \quad (3)$$

The water absorption (WA) test sample, measuring 50 mm × 50 mm × 10 mm, was weighed initially, soaked in room temperature water for 24 h, and drained, after which the final weight was determined to determine the water absorption. Eq. (4) provides the formula to calculate the water absorption.

$$\text{Water absorption } (\%) = \frac{Final\ weight - initial\ weight}{initial\ weight} \times 100\% \quad (4)$$

Additionally, test samples from the water absorption test were used to measure the thickness swelling. Before the sample was immersed in water, its thickness was measured. Next, the samples were allowed to soak in water at room temperature for 24 h, after which the thickness swelling (TS) was measured and determined using Eq. (5).

$$\text{Thickness swelling } (\%) = \frac{t \text{ after soaking} - t \text{ before soaking}}{t \text{ after soaking}} \times 100\% \quad (5)$$

The mechanical strength of the particleboard was analyzed using the modulus of rupture (MOR) to describe the capacity of the material to withstand loads. Testing was conducted using a universal testing machine (UTM Shimadzu, Kyoto, Japan) with MOR sample dimensions of 200 mm in length, 10 mm in thickness, and 50 mm in width and a crosshead speed of 10 mm/min. Eq. (6) was utilized to determine the MOR.

$$\text{MOR (MPa)} = \frac{3 \text{ Maximum load} \times \text{span length}}{2 \times \text{average width of speciment} \times (\text{average thickness of speciment})^2} \quad (6)$$

Furthermore, the modulus of elasticity (MOE) was tested on the same samples used for the MOR test. The deflection data were recorded during a particular load time. The formula used to calculate the MOE is Eq. (7).

$$\text{MOE (MPa)} = \frac{\Delta P L^3}{4 \Delta Y b h^3} \quad (7)$$

In which:

ΔP is the maximum load difference.

ΔY is the deflection that occurs in the difference in load.

L is the span length.

h is the average thickness of the specimen.

b is the average width of the specimen.

The internal bonding (IB) test utilized samples measuring 50 mm in length, 50 mm in width, and 10 mm in thickness with a crosshead speed of 2 mm/min. The surface area was calculated by considering the width and length of the test specimens. Subsequently, the steel beam was affixed to the test sample using epoxy adhesive and allowed to cure. Next, the test sample was positioned onto a universal testing machine (UTM), where the steel beam was subjected to tension perpendicular to the surface until reaching the maximum load (P). The IB strength was then calculated using Eq. (8).

$$\text{IB (MPa)} = \frac{\text{Maximum load}}{\text{surface area}} \quad (8)$$

2.6.5 Morphological Observation by Polarized Microscopy and Scanning Electron Microscopy (SEM)

The particleboard samples joined with citric acid-sucrose adhesive were sectioned into smaller pieces suitable for examination under a polarized microscope (Leica, Wetzlar, Germany). Due to the brittle nature of these samples upon cutting, scanning electron microscopy (SEM) analysis was not feasible. The prepared samples were mounted onto glass slides, and images were captured under 20× magnification, with adjustments made to brightness as necessary. On the other hand, the particleboard samples with attached ULEF-UF resin were cut into cross sections, affixed to carbon tape, and subjected to vacuum conditions for 72 h. Subsequently, images were acquired using a scanning electron microscope (SEM) equipped with a JEOL JSM 6100 instrument (JEOL Ltd., Tokyo, Japan) operating at 10 keV at magnifications of 50× and 250×.

2.6.6 Fire Properties of UL-94 and Torch Gas

UL-94, also recognized as the Underwriters Laboratories test standard UL-94, serves as a widely employed flammability assessment method for determining the relative flammability of composite

materials. This test evaluates, under controlled laboratory conditions, the ability of a composite part to self-extinguish once ignited, as well as its propensity to drip in response to exposure to a small open flame or radiant heat source. For the torch burn test, a standardized test sample measuring 50 mm in length × 50 mm in width × 10 mm in thickness was utilized. In accordance with BSN 1740:2008 [44], with slight modifications, particleboard samples treated with lignosulfonate phosphorus, lignosulfonate, and lignin or left untreated (control) were subjected to manual torching using a gas torch for a duration of 3 min (Fig. 1a). After the flame was extinguished, the weight of the sample, including the weight of the charred residue, was measured once more. Additionally, the initial vertical burning test involved exposing the particleboard to flame for 20 s, followed by observation and recording of the sample's appearance before and after contact with the fire (Fig. 1b).

(a) (b) (c)

Figure 1: Torch gas burning test (a), vertical burning test at 20 s (b), and vertical burning test at UL-94 (c) of particleboard bonded by ULEF-UF and citric acid-sucrose adhesives with lignin/lignosulfonate/phosphorylated lignin as the FR filler

A vertical burning test, conforming to the UL-94 standard (Serpong, Indonesia), was employed to assess the flammability of the materials (Fig. 1c). Test specimens measuring 125 mm × 13 mm × 12 mm were meticulously prepared for this evaluation. Methane gas served as the igniting agent and was applied to the sample for a duration of 10 s at a pre-established distance. Subsequently, the time taken (t) to extinguish the ignited flame was recorded. Based on the test results, the materials were classified as V-0 if they extinguished flames within 10 s without dripping, V-1 if they extinguished flames within 30 s without dripping, and V-2 if they extinguished flames within 10 s with dripping.

2.7 Formaldehyde Emission of Particleboards

Formaldehyde emission from the particle boards was measured using the Wilhelm Klaunitz Institute (WKI) bottle method as used by Ridho et al. [40], with a sample size of 25 mm in length and 25 mm in width. The sample was placed in a 500-mL WKI bottle containing 50 mL of distilled water, which was then placed in an oven set at 40°C for 24 h. A total of 10 mL of sample solution and formaldehyde standard solution series were placed into a 100-mL Erlenmeyer flask, and 10 mL of acetylacetone-ammonium acetate solution was added. The Erlenmeyer flask was then heated in a water bath (Joanlab water bath WB100-6, Huzhou, China) at 60°C–65°C for 10 min. The absorbance of each sample and standard solution was measured at a wavelength of 412 nm. The absorbance of the sample solution was

measured and plotted against the calibration curve of the formaldehyde standard solution to determine formaldehyde emission levels in the particleboard.

2.8 Statistical Analysis

A statistical analysis, one-way analysis of variance (ANOVA), was performed to observe the variability of the data (rheological properties, physical-mechanical properties and formaldehyde emission) with a confidence level of 95%. When the means were significant, a *post hoc* test by Duncan's test was carried out at the 5% level. IBM SPSS statistics v.26.0 (SPSS Inc., Chicago, IL, USA) was used for this analysis.

3 Results and Discussion

3.1 Physico-Chemical Properties of Modified Adhesives

The efficiency of the adhesive bonding system is governed by a variety of physicochemical features, which determine the adhesion processes, durability, and usability of the adhesive for various applications. The major physico-chemical features of adhesives include solids content, viscosity, pH, density, gelation time, and cohesion strength [45]. Table 3 summarizes the physico-chemical properties of the modified ULEF-UF and citric acid-sucrose adhesives. The solid content of neat ULEF-UF (PKUF) was greater than that of modified ULEF-UF (PUFL, PULFs, and PUFLsP). The solid content of an adhesive is the fraction of nonvolatile components (such as polymers, resins, and fillers). When organic fillers are added to an adhesive, the total solids content also increases. The amount of filler used directly influences the solids content of the adhesives. As the solids content increases, the adhesion strength also improves. This is because a larger solid content improves the cross-linking and bonding efficiency [41].

Table 3: Physicochemical properties of modified ULEF-UF and citric acid-sucrose adhesives

Adhesives	Solids content (%)	Viscosity (mPa·s)	pH	Density (g/cm^3)	Gel time (s)	Cohesion strength (kPa)
PKUF	61.93 ± 0.26^{a}	28.60 ± 0.14^{a}	6.29 ± 0.02^{c}	1.23 ± 0.01^{c}	547.02 ± 1.99^{d}	0.006 ± 0.00^{a}
PUFL	54.94 ± 2.71^{b}	12.44 ± 0.04^{d}	11.25 ± 0.02^{a}	1.29 ± 0.02^{b}	368.70 ± 0.56^{g}	0.002 ± 0.00^{d}
PUFLs	49.39 ± 0.07^{c}	11.69 ± 0.06^{e}	6.75 ± 0.03^{b}	1.30 ± 0.00^{ab}	423.00 ± 2.00^{f}	0.002 ± 0.00^{e}
PUFLsP	51.37 ± 0.71^{c}	27.89 ± 0.07^{b}	4.92 ± 0.03^{d}	1.31 ± 0.00^{a}	245.68 ± 1.18^{h}	0.006 ± 0.00^{b}
PASK	50.68 ± 0.27^{c}	9.57 ± 0.09^{f}	1.78 ± 0.01^{g}	1.16 ± 0.00^{e}	727.67 ± 2.52^{a}	0.002 ± 0.00^{f}
PASL	46.98 ± 0.30^{d}	13.31 ± 0.52^{c}	3.74 ± 0.01^{e}	1.19 ± 0.01^{d}	623.00 ± 1.00^{b}	0.003 ± 0.00^{c}
PASLs	44.00 ± 0.92^{e}	4.69 ± 0.04^{a}	2.10 ± 0.02^{f}	1.20 ± 0.00^{d}	607.34 ± 1.15^{c}	0.001 ± 0.00^{g}
PASLsP	42.34 ± 0.68^{e}	4.88 ± 0.20^{a}	1.63 ± 0.02^{h}	1.20 ± 0.00^{d}	543.35 ± 1.53^{e}	0.001 ± 0.00^{g}

Note: Different letters in the same column indicate significant differences.

In contrast, this study showed that post modification of ULEF-UF by the addition of lignin, lignosulfonate, and lignosulfonate phosphorus decreased the solid content by an average of 16.5%. This is probably due to the uneven distribution of lignin, lignosulfonate, and lignosulfonate phosphorus fillers in the ULEF-UF. In line with the solids content, the viscosity of ULEF-UF also decreased with the addition of lignin, lignosulfonate, and lignosulfonate phosphorus fillers. Controlling viscosity is critical for the ease of use and processing of adhesives. However, excessive filler loading might decrease the viscosity [46]. The viscosity of an adhesive can affect its ability to penetrate wood pores as well as its shelf life. This value surpasses the viscosity value specified in the standard (SNI 06-0060-1987) [47]. The shelf life of an adhesive decreases as its viscosity increases [48].

The gelation time of the adhesives was tested at 100°C, which is the time it takes for the adhesive to form a gel. The gelation time can also influence the adhesive's storage life. The greater the gelation time is, the longer the adhesive's shelf life [41]. Gelation is a result of the crosslinking of polymer chains inside the adhesive. Organic fillers can accelerate crosslinking, shortening the gelation time. The ULEF-UF adhesives rapidly solidify in acidic environments [49]. NH_4Cl is a frequently employed curing agent that facilitates the release of H+ ions by interacting with free formaldehyde in UF resin [50]. Furthermore, the density of the ULEF-UF adhesive increased with the addition of lignin, lignosulfonate, and lignosulfonate phosphorus fillers.

An adhesive's cohesion strength relates to its internal strength or its capacity to hold itself together under stress. The cohesion strength has a significant impact on the overall functioning of the adhesive bonding. Only a few fillers contribute considerably to the cohesive strength of the adhesive, such as talc, glass fiber, and mica [46]. In this study, the addition of lignin, lignosulfonate, and lignosulfonate phosphorus fillers did not increase the cohesion strength of the ULEF-UF or citric acid-sucrose adhesives. Greater adhesion strength in composite such as plywood is anticipated with a higher adhesive cohesion strength as reported in the study of Ridho et al. [40]. Several factors affect the cohesion strength, namely, the crosslinking density, curing temperature, and type and concentration of fillers [45].

Table 4 presents the statistical analysis of the adhesive properties. All adhesives had a significant effect at the 95% confidence level on the adhesive properties. Further analysis by *post hoc* tests was conducted to observe the effects of different adhesive types with filler on those properties. Filler and adhesive type had significant effects on the solid content, viscosity, pH, density, gel time and cohesion strength, as indicated by the different letters for the same observed parameters.

Table 4: One-way ANOVA of the adhesive properties and formaldehyde emission of the particleboard samples

Source	F value	Sig.
Solids content	95.723	0.000*
Viscosity	12,440.169	0.000*
pH	87,930.985	0.000*
Density	234.934	0.000*
Gel time	28,127.71	0.000*
Cohesion strength	22,691.323	0.000*
Formaldehyde emission	26.502	0.000*

Note: Asterisks indicates significant difference at confidence level 95%.

3.2 Thermal Gravimetric Analysis (TGA)

TGA evaluates the percent weight loss of a sample when it is heated uniformly in an acceptable atmosphere. The weight loss across various temperature ranges provides insights into the composition of the sample, including volatiles and inert filler, as well as indicators of thermal stability. The TGA and DTG spectra of citric acid-sucrose particleboard with lignin and modified lignin as filler are shown in Fig. 2. The composite weight loss based on temperature is shown in Table 5.

The weight loss of the samples can be divided into three stages: evaporation, degradation, and carbonation. During the evaporation stage, all types of samples lost between 2.82% and 3.61% due to the vaporization of water and volatile impurities from the specimens. At the degradation stage, the onset temperatures of the PASL (225.38°C) and PASL (223.71°C) samples increased compared to that of the

PASK sample (219.17°C). A similar observation was made for peak temperature, where PASL (296.83°C) and PASLs (292.67°C) had higher peak temperatures than did PASK (292.17°C), indicating that the addition of lignin and lignosulfonate made the citric acid-sucrose particleboards more thermally stable [51]. Moreover, after the addition of phosphorylated lignosulfonate, the peak temperature of the citric acid-sucrose particleboard (PASLSP) decreased to 278.18°C. However, the weight loss of the PASLSP group at this stage (51.81%) was lower than that of the PASLS group (55.05%). At 700°C, the remaining mass of the PASLSP (33.2%) was greater than that of the PASLS (29.73%). It should be noted that the addition of lignosulfonate and phosphorylated lignosulfonate did not significantly improve the heat resistance of the composite formed by sucrose and citric acid. However, the insertion of lignin may be favorable, as shown by its lower mass loss and higher peak temperature at the degradation stage.

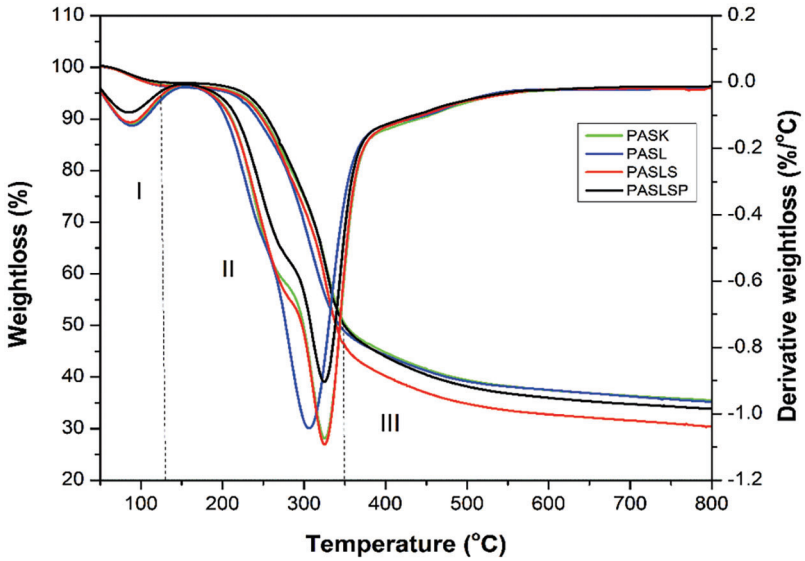

Figure 2: TGA and DTG curves of the citric acid-sucrose composite with lignin and modified lignin as filler

Table 5: Weight loss of laboratory-fabricated particleboard bonded with citric acid-sucrose

Step	Remark	PASK	PASL	PASLS	PASLSP
Evaporation	Temp_Onset (°C)	29.29	29.37	29.35	29.30
	Temp_Max (°C)	129.44	124.43	133.90	120.78
	Temp_End (°C)	189.90	191.40	199.40	180.67
	Weight loss (%)	3.45	3.61	3.60	2.82
Degradation	Temp_Onset (°C)	219.38	225.38	223.71	217.72
	Temp_Max (°C)	292.17	296.83	292.67	278.18
	Temp_End (°C)	375.42	353.74	385.42	383.58
	Weight loss (%)	50.04	48.13	55.05	51.81
Carbonation	Temp_stable (°C)	803.04	802.80	802.88	803.18
	Residue mass volatile at 700°C (%)	35.04	33.93	29.73	33.20

Fig. 3 shows the TGA and DTG spectra of the ULEF-UF-bonded particle boards, while the weight loss of the composites as a function of temperature is shown in Table 4. Similar to the results for the citric acid-sucrose composites shown in Fig. 2, the thermal decomposition of the ULEF-UF particle boards can be segmented into three stages with weight loss that recorded per stage has been summarized in Table 6. The evaporation step involved the loss of water and volatile impurities from the particleboard, where 3.02% to 4.16% of the water was lost at this stage. After the addition of lignin, lignosulfonate, and phosphorylated lignosulfonate, the peak temperature and weight loss of the particleboard experienced different extents of alteration. The addition of lignin decreased the peak temperature of the PUFL sample compared with that of the PKUF sample. However, its weight loss at the degradation stage was reduced to 47.72% compared to that of 54.20% in the PKUF samples. Similar observations were also made for the composite samples with added phosphorylated lignosulfonate (PUFLSP). With the addition of lignosulfonate (PUFLS) to the ULEF-UF particle boards, the peak temperature increased slightly to 277.51°C compared to 277.01°C for the PKUF samples, but the weight loss decreased slightly from 54.20% to 53.80%. At 700°C, the remaining masses of PKUF, PUFL, PUFLS, and PUFLSP were 26.66%, 29.96%, 27.28%, and 36.40%, respectively, indicating that the introduction of lignin and its derivatives improved the heat resistance of the particleboards. These findings are consistent with the conclusions of Lima Natarelli et al. [52], whereas in composite approaches to thermodynamic equilibrium, the thermal degradation process becomes more efficient. This is reflected in the decrease in activation energy. Lignin plays a crucial role in augmenting the overall thermal stability of particleboards. Collaboration between lignin and ULEF-UF in particleboards provides additional benefits, such as reducing resin utilization. This can enhance the efficiency and quality of the composite overall [52].

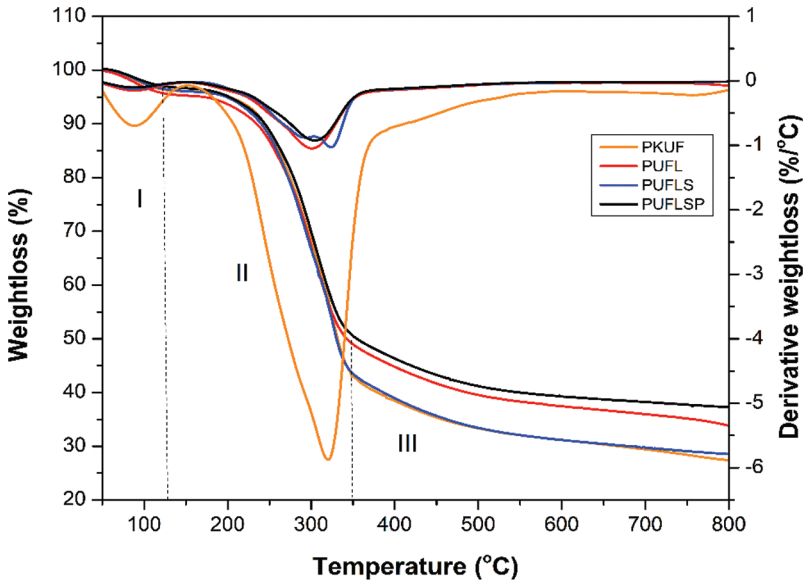

Figure 3: TGA and DTG of ultralow-emission urea formaldehyde particleboards with lignin and modified lignin as fillers

Table 6: Weight loss of laboratory-fabricated particleboard bonded with ULEF-UF

Step	Remark	PKUF	PUFL	PUFLS	PUFLSP
Evaporation	Temp_Onset (°C)	29.31	30.96	29.40	29.28
	Temp_Max (°C)	123.14	119.09	127.09	124.81

(Continued)

Table 6 (continued)

Step	Remark	PKUF	PUFL	PUFLS	PUFLSP
	Temp_End (°C)	172.91	171.91	173.75	171.75
	Weight loss (%)	3.62	4.16	3.58	3.02
Degradation	Temp_Onset (°C)	204.89	193.90	205.72	201.98
	Temp_Max (°C)	277.01	256.86	277.51	275.01
	Temp_End (°C)	356.48	358.11	357.11	358.60
	Weight loss (%)	54.20	47.72	53.80	47.38
Carbonation	Temp_stable (°C)	802.94	803.02	803.05	803.10
	Residu mass volatile at 700°C (%)	26.66	29.96	27.58	36.40

Compared with citric acid-sucrose particleboard, the addition of lignin seems to have more promising results in improving the thermal stability of ULEF-UF-bonded particleboard. This may be due to the different crosslinking effects between lignin and ULEF-UF compared to citric acid-sucrose. Lignin can crosslink with UF [53]. The thermal stability of the UF system has been improved by incorporating lignin [52]. Despite being able to crosslink with lignin [54], the crosslinking of citric acid-sucrose with lignin might not be as effective as that of ULEF-UF. This is probably the reason why the thermal stability of the citric acid-sucrose particleboard was not as prominent as that of its ULEF-UF-bonded counterparts after the addition of lignin. However, among the citric acid-sucrose composites, the addition of phosphorylated lignosulfonate led to the highest remaining mass at 700°C. Phosphorylation has been proven to improve the thermal stability of lignin [55]. Prieur et al. [56] reported that in their study, phosphorylated lignin can promote char formation by reacting with acrylonitrile butadiene styrene (ABS). Therefore, this may be the reason why a high residual amount can be observed in the composites with added phosphorylated lignosulfonate.

3.3 FTIR Analysis

In the infrared absorption spectrum of PASK (Fig. 4a), the band at 3343 cm^{-1} corresponded to the O-H stretching vibration, while the bands at 2918 cm^{-1} and 2865 cm^{-1} were attributed to the stretching vibration of C-H in methylene [57]. The weak band at 1726 cm^{-1} corresponds to the carbonyl groups present in esters [11], which are formed in the composite with citric acid-sucrose adhesive. The vibration of C = C is detected at 1632 cm^{-1}, indicating the interaction between citric acid and sucrose. Notably, the presence of anhydride in PASK was indicated by the development of C = C groups [58]. The weak peak at 1224 cm^{-1} and the strong peak at 1020 cm^{-1} represented the stretching of C-O in esters [59].

In the FTIR PASL spectrum, the intensity of the broadband peak at 3298 cm^{-1} increased due to O-H stretching, and an increase in the intensity of this peak suggested a prospective interaction between lignin and the adhesive, perhaps indicating the formation of hydrogen bonds between the hydroxyl groups in lignin and functional groups in the adhesive. Two small peaks attributed to C-H stretching appeared at 2918 cm^{-1} and 2849 cm^{-1}, and a peak attributed to C = O stretching in esters appeared at 1730 cm^{-1}. This peak implies the synthesis of ester bonds due to the reaction of carbonyl groups from the adhesive with the hydroxyl groups of lignin. Moreover, the peak resulting from the stretching of C = C shifted to 1600 cm^{-1}, and the peak at 1032 cm^{-1} was associated with aromatic C-H bending [60]. The intensities of all the peaks increased compared to those of the peaks present in PASK. This may be due to the presence of lignin in PASL. The spectrum of PASLS showed a stretching peak of O-H at 3318 cm^{-1}, with only

one small peak at 2918 cm^{-1} representing the stretching vibration of C-H in methylene, a weak band at 1726 cm^{-1} indicating carbonyl groups present in esters, a weak peak at 1612 cm^{-1} caused by the vibration of the aromatic framework, probably arising as a result of interactions between lignosulfonate and the adhesive, and a strong peak at 1026 cm^{-1} belonging to aromatic C-H bending in-plane deformations. The intensity of this peak signifies the presence of aromatic rings, probably from the interaction of lignosulfonate with the adhesive. The peak at 1232 cm^{-1} in the lignosulfonate spectrum is characteristic of the guaiacyl (G) ring present in lignin derived from softwood [60].

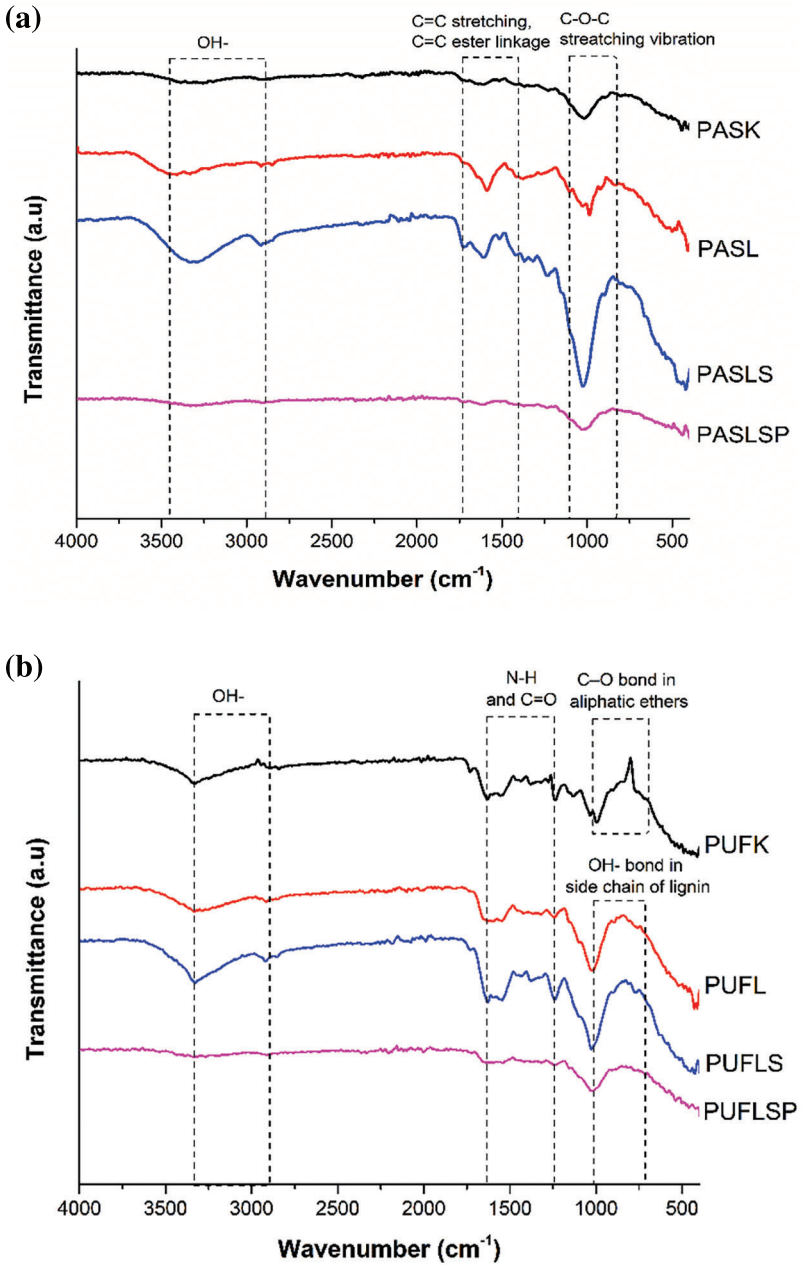

Figure 4: (a) FTIR of citric acid-sucrose particleboard without lignin (PASK), with lignin (PASL), with lignosulfonate (PASLs), with lignosulfonate phosphorus (PASLsP), (b) ULEF-UF particleboard without lignin (PUFK), with the addition of lignin (PUFL), lignosulfonate (PUFLs), and lignosulfonate phosphorous (PUFLsP)

In the FTIR spectrum of PASLSP, the stretching vibration peak of O-H appears at 3326 cm^{-1}, and the intensity of this peak decreases after phosphorylation [56]. The weak band at 2906 cm^{-1} was attributed to the stretching vibration of C-H in methylene [45], and the weak peak at 1730 cm^{-1} was caused by the stretching vibration of C = O in the ester form due to the combination of sucrose and citric acid in PASLSP [58]. This result is then compared with the FTIR spectrum of PASLS, where the weak peak resulting from the vibration of the aromatic framework shifted to 1616 cm^{-1}. This shift in the peak is due to changes in the aromatic structures, possibly from the interaction of phosphorylated lignosulfonate with the adhesive, and the strong peak at 1032 cm^{-1} was associated with aromatic C-H in-plane deformations. The peak at 1232 cm^{-1} in the lignosulfonate spectrum was characteristic of the G ring present in softwood lignin [60].

Fig. 4b presents the FTIR spectrum of particleboard bonded with ULEF-UF resin along with lignin and its modified forms. A broad yet relatively sharp peak associated with O-H and N-H hydrogen-bonded groups appeared at 3334 cm^{-1} [61]. Peaks at 2890 cm^{-1} and 2845 cm^{-1} corresponded to the Fermi resonance of $-CH_3$, symmetric stretching vibrations of $-CH_2$ or $-CH_3$, and anti-symmetric stretching vibrations of $-CH_2$ [62]. The weak band at 1730 cm^{-1} corresponded to the stretching of −CO in formaldehyde [63], the two peaks at 1632 cm^{-1} were related to the stretching of C = O in the primary amide, and the weak peak at 1521 cm^{-1} represented the stretching of C-N and N-H bending vibrations in the secondary amide [64]. The weak peak at 1440 cm^{-1} was associated with methylene bridges [65], 1375 cm^{-1} represented the bending vibration of C-H in secondary amides, and the weak peak at 1240 cm^{-1} was the stretching vibration of C-N and N-H in tertiary amides [66]. The presence of monomethylol urea in UF was indicated by the band at 1130 cm^{-1}, which is associated with C-O-C bonds [67]. According to Myers [68], the bands spanning from 1020 cm^{-1} to 1050 cm^{-1} may represent amides in the resins due to C-N stretching from C-N or C-N2. Therefore, either methylene urea or methylated urea could be the cause of these bands [66], and the strong band at 1000 cm^{-1} was attributed to the stretching of C-O from methylol groups [68].

The FTIR spectrum of PUFL contains the same broad band for O-H and N-H groups. The C–H stretching vibrations of methylene, methyl and methoxyl groups on the side chains are responsible for the weak peak at approximately 2906 cm^{-1} [69], and the peak at 1628 cm^{-1} is due to C = O stretching in the primary amide. The intensity of this peak increases due to the presence of lignin [70], and the vibration of C = C planar deformation in aromatic rings is responsible for the peak at approximately 1547 cm^{-1}. Compared to that of PUFK, the peak at 1130 cm^{-1} due to monomethylol urea is absent in PUFL, and the intensity of the band from 1020 cm^{-1} to 1050 cm^{-1} increases in the case of PUFL. Additionally, the bands attributed to hydroxyl and N-H groups are sharper in the FTIR spectrum of PUFLS than in those of PUFK and PUFL. Additionally, the peaks attributed to the Fermi resonance of $-CH_3$, the symmetric stretching vibration of $-CH_2$ or $-CH_3$, and the anti-symmetric stretching vibration of $-CH_2$ appear at 2890 cm^{-1} and 2845 cm^{-1}, possibly due to the presence of lignosulfonate in the adhesive system. The peak for the O-H and N-H groups in PUFLSP had the lowest intensity and appeared at 3334 cm^{-1}. The C-H stretching vibrations of methylene, methyl, and methoxyl groups on the side chains were responsible for the weak peak at approximately 2918 cm^{-1} [69], the weak peak at 1240 cm^{-1} attributed to C-N and N-H stretching in tertiary amides [66], and the intensity of all the peaks in the FTIR spectrum of PUFLSP decreased due to phosphorylation.

3.4 Morphological Observation

Fig. 5 shows the morphology analysis of the particleboard bonded by sucrose-citric acid and ULEF-UF resin using a polarized microscope. Because of the compact and nonbrittle structure of the particleboard, further observation via SEM (Fig. 6) was limited to the cross-sectional surface bonded by ULEF-UF.

Fig. 5 shows that the citric acid-sucrose- and ULEF-UF adhesives appeared on the surface of the particles even though only superficial surface scanning was performed. Similar findings were also described by Nuryawan et al. [71]. Furthermore, some agglomeration spots were found on the surface of the particleboard. Citric acid-sucrose may not fully interact with particles during board preparation. Del Menezzi et al. [72] reported that when citric acid and wood combine, they form a bond line with a deep brown color. This reaction can be triggered by the oxidation of the wood's contents caused by heat and citric acid. This may also result from the reactivity of lignin, carbohydrates, and their model compounds with citric acid.

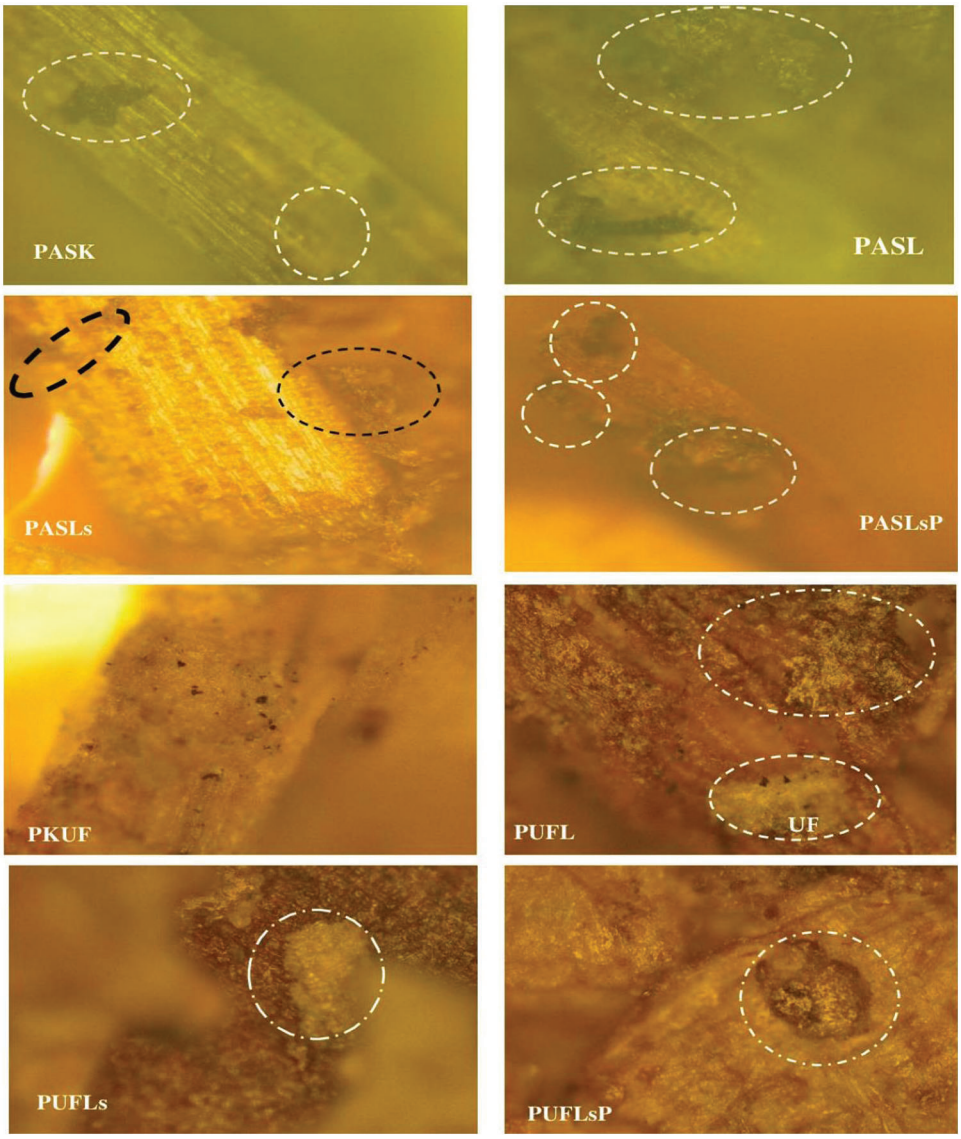

Figure 5: Microscopic observation by polarized microscopy on citric acid-sucrose particleboard without lignin (PASK), with lignin (PASL), with lignosulfonate (PASLs), with lignosulfonate phosphorus (PASLsP) and on low-emitting UF particleboard without lignin (PUFK), with lignin (PUFL), with lignosulfonate (PASLs), and with lignosulfonate phosphorous (PASLsP)

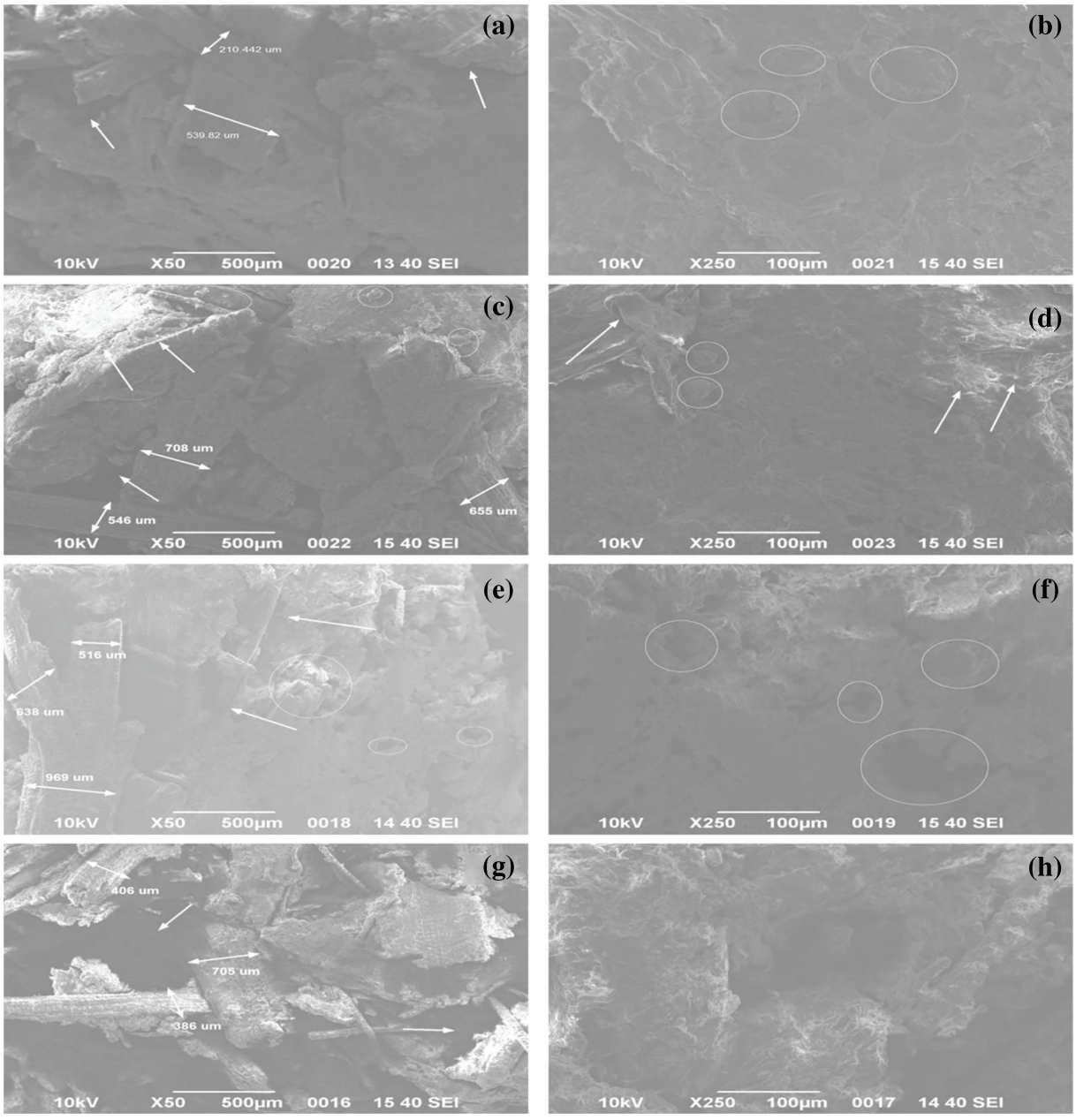

Figure 6: (a and b) show SEM images of the ULEF-UF composite at 50- and 250-fold magnification, respectively; (c and d) show SEM images of the UF composite with lignin at 50- and 250-fold magnification; (e and f) show SEM images of the ULEF-UF composite with lignosulfonate at 50- and 250-fold magnification; and (g and h) show SEM images of the ULEF-UF composite with lignosulfonate phosphorus at 50- and 250-fold magnification, respectively

The addition of lignin/lignosulfonate/lignosulfonate phosphorous to adhesives results in a new agglomeration on the board surface. The conditions or techniques for complying with resin-containing lignin and its derivatives may not yet be optimal. A white crystal clump on the surface of the ULEF-UF-bonded board could be the result of the ULEF-UF resin, which does not react well with lignin. A white

crystal clump on the surface of the UF-bonded board may be caused by the ULEF-UF resin, which does not react well with lignin. Although some studies have shown that citric acid can react with hydroxyl groups in biomass components to increase bond strength [11,72,73], it has been suggested that sucrose caramelization is promoted by heating during the pressing step [74].

The ULEF-UF particleboard has an irregular shape, as shown in Fig. 6, and image (a) shows a UF composite at 50× magnification; it displays a large number of aggregates and flattened plate-like crystals, and rounded granular surface growth in a portion of the area is evident. On the other hand, image (b) of the UF composite at 250× magnification shows that the surface of the sphere-shaped particles was covered with many holes and wrinkles. Plate-like crystals are proposed to denote the progressive or full-growth form of crystals. Formaldehyde and moisture evaporation are what cause the tiny holes on the surface. Numerous sphere-shaped particles may be seen in image (c), along with some spherical particles arranged linearly in groups.

On the other hand, the morphology of the ULEF-UF particleboard without lignin was completely opposite to that of the ULEF-UF particleboard without lignin; wrinkles and holes decreased when the ULEF-UF particleboard was treated with lignin at the same time. The addition of lignin may theoretically increase the intramolecular interactions of the composite and gradually increase its flexibility [75], and lignin microfibers are firmly grasped and arranged in bunches in relation to one another. The presence of compact bundles is explained by the presence of lignin.

In comparison to the surface of the untreated particleboard, which has many primary particles that resemble snowflakes, leading to the development of featureless and fibrous crystals exhibiting a greater degree of advancement, lignin clearly affects the ULEF-UF particleboard, and the development of many spherical networks in the fractured area may indicate interactions between the ULEF-UF particleboard and lignin. The width of the fibrous particles increased as a result of lignin addition; usually, the particles of lignosulfonate are hollow and round, and the interaction of lignosulfonate with the ULEF-UF adhesive may result in aggregation and dispersion within the adhesive matrix. This can have an effect on the distribution of lignosulfonate particles within the matrix, thus influencing the overall morphology of the composite. The ULEF-UF particleboard with lignosulfonate had slightly larger particle diameters, as shown in image (e). The presence of lignosulfonate causes more cross-linking in the ULEF-UF particleboard, which leads to additional aggregation [67]. A dynamic macromolecular network structure was created, which improved the hardness and durability. This demonstrates how the lignosulfonate modification increased the strength of the composite. Image (f) shows a ULEF-UF-particleboard with lignosulfonate at 250× magnification, which has a significant amount of small spherical particles. The more intricate cross-linked network structure of the composites was primarily responsible for the spherical particle production [76]. In an SEM image of ULEF-UF lignosulfonate phosphorus, certain crystals appear needle-like on the surface, and due to typical elastic failure, the fractured interfaces of the composite exhibited prominent wrinkle and waveform patterns. SEM image (h) of the ULEF-UF-composite with lignosulfonate phosphorus at 250× magnification revealed the crystal lattice and the presence of pores on the surface due to the intrinsic stiffness of the composite. The surface of the composite roughened and thickened, suggesting that the hardness increased.

3.5 XRD Analysis

Like woody biomass, the areca leaf sheath has a high cellulose content of 66.08%, lignin content of 19.59%, hemicellulose content of 7.4%, and content of other compounds, such as pectin, wax, fat, extractives, and pectin [77]. In terms of crystallinity measurements, cellulose consists of a crystalline structure and a noncrystalline segment within this linear linkage. The cellulose was made of D-glucopyranose units linked by β-1,4-glycosidic bonds [78]. Table 7 shows the degree of crystallinity for

the different particleboard samples produced in this work. The degree of crystallinity does not differ significantly and follows a similar pattern depending on the resin type and filler used in particleboard production. Based on lignin characteristics, after three washing treatments, the Eucalyptus lignin has more syringyl (S) units than G units, with an S/G ratio of 4.49, making it more reactive [27]. Furthermore, rich G lignin (such as Chinese kraft lignin) makes it difficult to disperse biomass particles and UF [79]. Except for PASL, the addition of filler resulted in reduced crystallinity, with the particleboard with sucrose-citric acid having slightly lower crystallinity than the ULEF-UF boards.

Table 7: Degree of crystallinity of particleboard bonded with ULEF-UF resin or citric acid-sucrose adhesives

Particleboard types	Degree of crystallinity (%)
PUFK	36.04
PUFL	35.59
PUFLs	31.19
PUFLsP	32.08
PASK	35.54
PASL	39.90
PASLs	30.28
PASLsP	29.47

Cellulose swelling may occur, disrupting the crystalline region of cellulose to some extent and lowering crystallinity [80]. Furthermore, the reduction in crystallinity is presumably ascribed to the inclusion of lignin or its derivatives, particularly in the amorphous fraction. Additives such as lignin, lignosulfonate, phosphorus, or solvents (water and NaOH) are added to lignocellulose biomass, such as areca leaf particles, and the additives enter the amorphous fraction first [80]. Lignosulfonate is more hydrophilic than lignin, influencing its ability to easily bind with OH in cellulose particles to form hydrogen bonds [81]. Like lignosulfonate, lignosulfonate phosphorous is expected to be more hydrophilic considering the presence of hydrophilic sulfonate groups on the lignosulfonate structure [82]. In addition, the incorporation of ammonium lignosulfonate (ALS) results in better working performance with UF than with Chinese and Brazilian kraft lignin and sugar bagasse lignin [79].

In the case of citric acid-sucrose, an ester linkage was formed (as confirmed by the FTIR spectra, Fig. 4a) between the OH in the cellulose molecules and citric acid. Similar findings with proposed ester linkage formation between citric acid and −OH from cellulose and sucrose were previously reported [80]. The board strength may be impacted by periodic rearranging of the chemical chain in the amorphous sections [12,80].

A prior report on particleboard bonded with sucrose and citric acid as an adhesive showed that the particleboard strength had a relationship with the crystallinity based on its diffractogram [80]. However, in this study, the decrease in crystallinity did not increase the mechanical strength (MOE, MOR, or IB), as found in a study by Liao et al. [80] using sucrose-citric acid adhesives to prepare bagasse particleboard. Differences in the raw material characteristics (extractives, pectin, wax, and fat, in addition to chemical components), particle size, particleboard processing conditions, and adhesive level, as well as the addition of lignin and modified lignin, may influence these differences.

3.6 Mechanical and Physical Properties and Formaldehyde Emission of Particleboards

Table 8 displays the one-way ANOVA results for the impact of different adhesive types on the characteristics of the particleboard. The choice of adhesive used has a substantial impact on all the tested

properties of the particleboard, except for the moisture content. A *post hoc* test, specifically the Duncan test, was conducted to further differentiate the average values. The outcomes of this test can be found in Table 9.

Table 8: One-way ANOVA of the mechanical and physical properties of the particleboards

Source	F value	Sig.
Moisture content	1.003	0.492
Density	6.234	0.010*
Thickness swelling (TS)	19.900	0.000*
Water absorption (WA)	9.914	0.002*
Modulus of elasticity (MOE)	9.300	0.003*
Modulus of rupture (MOR)	60.852	0.000*
Internal bond strength (IB)	137.295	0.000*

Note: Asterisks indicate significant difference at confidence level of 95%.

Table 9: Physical and mechanical properties of the laboratory-fabricated particleboards bonded with ULEF-UF resin, citric acid-sucrose, and filler

Particleboard types	MC (%)	Density (g/cm^3)	TS (%)	WA (%)	MOE (MPa)	MOR (MPa)	IB (MPa)
PKUF*	8.81 ± 0.13^{a}	0.84 ± 0.01^{a}	93.73 ± 0.14^{bc}	153.03 ± 1.05^{b}	81.64 ± 8.51^{b}	7.82 ± 0.74^{c}	0.64 ± 0.01^{b}
PUFL*	9.21 ± 0.11^{a}	0.85 ± 0.01^{a}	74.34 ± 0.20^{d}	135.42 ± 0.61^{bc}	74.24 ± 19.63^{bc}	8.80 ± 1.43^{bc}	0.67 ± 0.03^{b}
PUFLs*	8.99 ± 0.23^{a}	0.82 ± 0.03^{ab}	85.33 ± 0.73^{cd}	140.66 ± 0.03^{bc}	72.40 ± 8.52^{bc}	9.34 ± 0.21^{b}	0.68 ± 0.00^{b}
PUFLsP	7.36 ± 0.528^{a}	0.84 ± 0.01^{a}	108.85 ± 0.64^{ab}	137.16 ± 0.13^{bc}	103.70 ± 0.79^{a}	12.26 ± 0.86^{a}	2.62 ± 0.21^{a}
PASK	8.16 ± 0.39^{a}	0.75 ± 0.01^{c}	53.38 ± 0.14^{de}	124.09 ± 1.48^{bc}	63.95 ± 4.55^{bcd}	4.16 ± 0.25^{d}	0.09 ± 0.06^{c}
PASL	6.95 ± 0.04^{a}	0.75 ± 0.01^{c}	69.28 ± 0.89^{cd}	152.86 ± 1.77^{b}	43.27 ± 6.57^{d}	3.72 ± 0.70^{d}	0.07 ± 0.05^{c}
PASLs	6.75 ± 0.36^{a}	0.83 ± 0.04^{ab}	51.49 ± 0.41^{a}	110.04 ± 1.26^{c}	49.27 ± 5.54^{d}	4.07 ± 0.15^{d}	0.10 ± 0.05^{c}
PASLsP	10.80 ± 0.07^{a}	0.78 ± 0.04^{bc}	122.28 ± 1.71^{e}	211.66 ± 2.40^{a}	52.78 ± 6.71^{cd}	1.32 ± 0.00^{e}	0.02 ± 0.00^{c}

Note: The data marked with asterisks were adapted with permission from Madyaratri et al. [24]. Copyright ©2022, MDPI. Different letters in the same column indicate significant differences.

Table 9 illustrates the mechanical and physical strengths examined in this study. The moisture content of the ULEF-UF-bonded boards ranged from 7.36% to 9.21%, whereas for the particleboards fabricated with citric acid-sucrose as a binder, the moisture content varied between 6.75% and 10.80%. The density of the ULEF-UF particle boards (0.82 to 0.85 g/cm^3) exceeded that of the citric acid-sucrose composites (0.75 to 0.83 g/cm^3). Compared with the ULEF-UF boards, the citric acid-sucrose composites exhibited lower TS values ranging from 51.49% to 122.28% (TS values from 74.34% to 108.85% for the ULEF-UF boards), indicating the slightly better dimensional stability of the citric acid-sucrose particleboard, except for those with added phosphorylated lignosulfonate (PASLsP). Regarding water absorption (WA), a similar pattern was noted, with the citric acid-sucrose composites exhibiting generally lower WA values, except for PASLsP. Among all the particleboard samples, the PASLs (with added lignosulfonates) exhibited significantly better dimensional stability, as evidenced by their having the lowest TS and WA compared to the other particleboard samples.

Citric acid-bonded composites frequently demonstrated better dimensional stability than ULEF-UF bonded particleboard, most likely due to the low moisture sensitivity of citric acid [83]. UF is well known for being highly susceptible to hydrolysis when exposed to moisture [84]. In this study, the

addition of lignin, lignosulfonate, and phosphorylated lignosulfonate resulted in varying degrees of TS and WA of the composite. The addition of lignin and lignosulfonates to the ULEF-UF particleboard improved its dimensional stability, as evidenced by the lower TS and WA values. Moreover, adding lignosulfonates to a citric acid-sucrose composite improved the dimensional stability of the material, as shown in the literature [85]. However, the addition of phosphorylated lignosulfonate considerably reduced the dimensional stability of both particleboards. This could be because phosphorylated lignosulfonates are more water soluble than other lignosulfonates. Therefore, it is more likely to be dissolved in water, resulting in more empty voids in the composites and making water penetration relatively easy [24].

The addition of phosphorylated lignosulfonate substantially enhanced the mechanical properties of the ULEF-UF composite. ULEF-UF particleboards with phosphorylated lignosulfonate had a greater MOE, MOR, and IB than did the ULEF-UF composite or the ULEF-UF composite manufactured with the addition of lignosulfonate and lignin. This could be because phosphorylated lignosulfonate has higher reactivity, which could improve its compatibility with UF resin. On the other hand, the introduction of lignin and its derivatives had a mixed effect on the MOR, IB, and MOE values of citric acid-sucrose particleboards. Although there have been reports indicating that the hydroxyl groups on the aliphatic chains of lignin units are capable of undergoing reactions with citric acid [72], additional research is necessary to clarify the relationships between citric acid, sucrose, and lignin.

Table 10 shows the formaldehyde emission of the particleboards bonded by citric acid-sucrose and ULEF-UF with filler addition. The use of commercial UF adhesive as a particleboard resulted in formaldehyde emissions between 0.79 and 0.94 mg/L [86]. Compared with emissions released by particleboard, ULEF-UF has lower formaldehyde emissions when using UF resin with a formaldehyde/urea mole ratio of 0.95, which is also categorized as an emission class of F**** (very low concentration). According to JIS A 5908-2003 [43], the results of formaldehyde emission testing on citric acid-sucrose and ULFE-UF with lignin and modified lignin as filler fall into the F**** category, which is <0.4 mg/L. Compared with the formaldehyde content of particleboard bonded by UF with phenolated lignin at various percentages, this content is lower [69]. The addition of lignin, lignosulfonate and phosphorylated lignosulfonate has a positive effect on reducing formaldehyde emission, as indicated by the decreased emission of the particleboard without filler. Previous studies have shown that the modification of UF adhesives with fillers such as lignin or nanolignin is one approach for reducing formaldehyde emission [40,87]. The process involves adding formaldehyde to the phenolic hydroxyl groups found in lignin, resulting in the formation of methylene bridges between the lignin molecules [40].

Table 10: Formaldehyde emission of particleboards bonded with citric acid-sucrose and ultralow formaldehyde emission-urea formaldehyde with filler addition

Adhesives	Formaldehyde emission (mg/L)	JIS A 5908-2003 (mg/L)
PKUF	0.141 ± 0.004^{bc}	Maximum 0.4 (F****)
PUFL	0.113 ± 0.004^{ef}	Maximum 0.4 (F****)
PUFLs	0.124 ± 0.015^{de}	Maximum 0.4 (F****)
PUFLsP	0.103 ± 0.008^{f}	Maximum 0.4 (F****)
PASK	0.094 ± 0.004^{a}	Maximum 0.4 (F****)
PASL	0.130 ± 0.005^{cd}	Maximum 0.4 (F****)
PASLs	0.135 ± 0.003^{bcd}	Maximum 0.4 (F****)
PASLsP	0.144 ± 0.002^{b}	Maximum 0.4 (F****)

Note: Different letters in the same column indicate significant differences.

Citric acid-sucrose particleboards without any additives contain formaldehyde. As reported before, some wood species contain formaldehyde [88], which might be due to the thermal degradation of polysaccharides in the wood [89,90]. However, the citric acid-sucrose particleboard tended to result in greater formaldehyde emission than predicted, even though it is included in the level criteria of F**** based on the JIS A 5908-2003 classification, which might be a citric acid-sucrose reaction with ALS particles that causes the separation of formaldehyde in the ALS and leads to high formaldehyde emission under acidic conditions. Two lignin positions are side-chain units containing primary alcohol, and the carbonyl group in the β position is prone to formaldehyde [90]. Furthermore, formaldehyde comes from the main wood components, such as cellulose, lignin and hemicellulose, which are also extracted, and lignin is considered to contain more formaldehyde than carbohydrates [90].

Statistical analysis (Table 4) revealed that the adhesive and filler type significantly influenced the formaldehyde emission of the particleboard at a confidence level of 95% (0.00). The formaldehyde emission of the particleboard bonded with ULFE-UF significantly differed from that of citric acid-sucrose. Post hoc tests indicated that the properties of PKUF and PASK were significantly different from those of particleboard with filler. PUFLs have different formaldehyde emission levels than PUFLsP, while the emission levels of PASLsP are also significantly different from those of PASL and PASLs.

3.7 Fire Properties of the Particleboard

Torch burn tests and UL-94 were used to evaluate the fire resistance ability of the particleboard, and the results are presented in Tables 11 and 12. Fig. 7 shows the performance of the particleboard produced in this study after a fire test for 20 s. According to a similar fire test, particle board-bonded citric acid-sucrose has a different behavior than particle board-bonded ULEF-UF. Smoldering combustion with smoke has only been found in particleboard with citric acid-sucrose. Chemical reactions are intrinsically linked to mass transfer and heat processes in smoldering combustion [91]. However, further in-depth investigations are needed to understand the underlying reason. As reported before, smoldering combustion, often encountered in the burning of porous fuels at low temperatures, occurs slowly and without flames. This phenomenon is frequently observed in peatlands, where polyurethane foam and charred cellulosic insulation are combusted when heated. Smoldering combustion is a major contributor to household fires, warranting attention and oversight for safety in commercial and aerospace flights, as well as industrial environments [92].

Table 11: Fire test on areca palm leaf particleboard using a gas torch for 3 min

Treatment	Initial weight (g)	Post-flame weight (g)	Mass loss (%)
PKUF*	15.99	11.29	29.39
PUFL*	15.78	4.52	71.36
PUFLs*	17.62	12.38	29.74
PUFLsP	23.87	13.83	42.05
PASK	18.13	2.83	85.13
PASL	18.23	7.41	59.30
PASLs	18.87	9.7	48.44
PASLsP	23.87	13.83	42.05

Note: The asterisk indicates data adapted with permission from Madyaratri et al. [24].Copyright ©2022, MDPI.

Table 12: Classification of fire resistance of UL-94 areca particleboard

Sample	Post-flame duration (s)	Duration for fire suppression (s)	Melting	Grading
PKUF*	0	0	No	V-0
PUFL*	0	0	No	V-0
PUFLs*	0	0	No	V-0
PUFLsP	0	0	No	V-0
PASK	0	13 ± 4	No	V-0
PASL	0	10 ± 1	No	V-0
PASLs	0	9 ± 4	No	V-0
PASLsP	0	0	No	V-0

Note: The asterisk indicates data adapted with permission from Madyaratri et al. [24]. Copyright ©2022, MDPI.

Figure 7: Particleboard before and after the vertical fire test for 20 s: ULEF-UF particleboard (PKUF), ULEF-UF particleboard with lignin (PuFL), ULEF-UF particleboard with lignosulfonate (PUFLs), ULEF-UF particleboard with lignosulfonate phosphorus (PUFLsP), citric acid-sucrose particleboard (PASK), citric acid-sucrose particleboard with lignin (PASL), citric acid-sucrose particleboard with lignosulfonate (PASLs), and citric acid-sucrose particleboard with lignosulfonate phosphorus (PASLsP)

The test results in Table 11 are the weight loss of the samples after combustion. Fig. 7 shows that almost one-third of the control PKUF samples were burned after the fire was extinguished, which corresponds to a 29.39% weight loss, as shown in Table 11. After the addition of lignosulfonate (PUFLs) and phosphorylated lignosulfonate (PUFLsP), the areas of burning and fire spreading seemed to be less severe than those of the PKUF samples. However, weight losses of 29.74% and 42.05%, respectively, were recorded. Moreover, for the PUFL samples, the burnt area and spreading of fire seemed to be more or less the same as those of the control PKUF samples. However, the PUFL samples experienced a weight loss of 71.36% after burning. This suggests that while the addition of lignin may have prevented the fire from spreading across the sample surface, it did not shield the sample from losing weight as a result of the fire.

On the other hand, the control citric acid-sucrose particleboard (PASK) almost completely burned after being manually tested for fire resistance with a gas torch, whereas the particleboard treated with lignin solution lost 59.3% of its original weight. Moreover, the initial weight of the particleboard treated with the lignosulfonate solution decreased to 48.44%. The appearance of the particleboard after burning can be observed in Fig. 7, in which the PASK samples were almost completely burned, indicating that the citric acid and sucrose did not have any fire resistance. This demonstrates that the insertion of lignin and lignosulfonate increases the fire resistance of citric acid-sucrose particleboard. The weight loss of the particleboard with lignin and lignosulfonate was less than that of the particleboard without these additives. The addition of lignosulfonate increases the combustion residue of particleboard more than does the addition of lignin, as Madyaratri et al. [24] found that lignosulfonates have superior fire resistance and stability compared to lignin.

In addition, the vertical fire resistance of the particleboard was tested using the UL-94 method. The UL-94 method is a straightforward technique used in industry. Material testing is performed in the vertical direction (V). The UL-94 test is utilized for assessing fire resistance characteristics, with flammability samples categorized as V-0, V-1, or V-2 [93] denoting high, medium, or minimal flammability levels, respectively The overall fire resistance of the particleboard received a V-0 rating in UL-94 (Table 12). The addition of lignin or lignosulfonate solution had no significant effect on the fire resistance.

Based on the test results, the time for fire extinguishing was further reduced by treatment with lignin and lignosulfonate. The particleboard samples exhibited lower flammability with shorter times required for the fire to be extinguished. It is plausible that the fire resistance of the material improves through conversion into particleboard, albeit the outcomes are still inferior to those of previous research by Madyaratri et al. [27]. Their study on the treatment of lignin and lignosulfonate on ULEF-UF adhesive areca leaf sheath particleboard achieved a V-0 grading in the UL-94 classification, requiring less time for fire suppression. This discrepancy might be attributed to the superior interaction between lignin or lignosulfonate and ULEF-UF compared to citric acid-sucrose as an adhesive with the same particle material. However, further research is required to validate this phenomenon.

4 Conclusions

In this study, lignin, lignosulfonate, and phosphorylated lignosulfonate were introduced as biobased additives in particleboard bonded with citric acid-sucrose compared to ULEF-UF resin. The incorporation of these lignin variants into the adhesive system had varying impacts on the properties of the particleboard, and these effects differed between citric acid-sucrose and ULEF-UF-bonded particleboards. Notably, the integration of lignin seems to have a more pronounced effect on the thermal characteristics of ULEF-UF-bonded particleboard, likely due to the enhanced compatibility between the ULEF-UF resin and lignin. This was supported by morphological observations through SEM and polarized microscopy, where the aggregation of resin and lignin/lignosulfonate/lignosulfonate phosphorus was less apparent on the surface of the ULEF-UF-bonded boards than on the surface of the citric acid-sucrose bonded particle boards. The smoldering combustion of particle boards bonded by citric acid-sucrose is an important

finding, and the scientific background of the interaction between adhesives and chemical components, including those in the areca leaf sheath and filler (lignin/lignosulfonate/lignosulfonate phosphorus), needs to be investigated. Regarding the mechanical and physical features, the addition of phosphorylated lignosulfonate significantly improved the mechanical quality of the ULEF-UF-bonded boards but concurrently slightly compromised the dimensional stability of the boards. Conversely, the addition of a lignin or lignosulfonate solution did not exert a significant impact on the fire resistance of the modified particleboard, although it did enhance the flammability of the citric acid-sucrose bonded particleboard. Overall, the introduction of lignin and lignosulfonate solutions did not yield a consistent trend in the properties of the particleboard. Based on the study's findings, it can be concluded that lignosulfonate is the best filler for both ULEF-UF and citric acid-sucrose resins, although it is not as effective as phosphorylated lignosulfonate in terms of enhancing fire resistance. Particleboard with added lignosulfonate exhibited enhanced dimensional stability and mechanical strength, whereas phosphorylated lignosulfonate had a detrimental effect on these properties. Further research is needed to explore the underlying reasons for these observed variations.

Acknowledgement: This research was supported by the project "Development, Exploitation Properties and Application of Eco-Friendly Wood-Based Composites from Alternative Lignocellulosic Raw Materials", Project No. НИС-Б-1290/19.10.2023, carried out at the University of Forestry, Sofia, Bulgaria. The authors are grateful for the postdoctoral program (Grant Number: 86/II/HK/2023) of the National Research and Innovation Agency (BRIN) for Puji Rahmawati Nurcahyani and the research assistant scheme (Grant Number: 8/HK/II/2024) of BRIN for Dewi Shafa Kayla. The authors would like to thank Erika Ayu Agustiany, M. Si, and Muhammad Rasyidur Ridho, M. Si for their help in preparing the FTIR, TGA, and XRD images. Authors also thank to Henri Vahabi for facilitating in using the laboratory and equipment during Séjour Scientifique de Haut Niveau (SSHN) program at 15 November–31 December 2023 in Laboratoire M.O.P.S., Université de Lorraine France. The authors would like to thank the facilities and services involved in conducting the research at the Integrated Laboratory for Bioproducts (ILaB) BRIN through the E-Layanan Sains BRIN, Indonesia.

Funding Statement: This work was funded by the Equity Project Universitas Sumatera Utara (Number: 10/UN5.2.3.1/PPM/KPEP/2023), which is entitled Pengembangan Papan Partikel Tahan Api Rendah Emisi Berbahan Limbah Tanaman Mangrove dan Limbah Tanaman Pertanian Melalui Penambahan Lignin Terfosforilasi Sebagai Filler. PT Greenei Alam Indonesia (PT GAI) contributed to providing the areca leaf sheath through the implementation of a collaboration agreement with the Research Center for Biomass and Bioproducts BRIN FY 2023-2025.

Author Contributions: Apri Heri Iswanto, Widya Fatriasari, Lee Seng Hua, Petar Antov, Asma Sohail: conceptualization, writing—original draft, and writing—review and editing; Linda Makovická Osvaldová, Sarah Latifah, Lum Wei Chen, and Sukma Surya Kusumah: methodology and validation; Dewi Shafa Kayla, Linda Makovická Osvaldová, Sukma Surya Kusumah, Apri Heri Iswanto, Widya Fatriasari, Lee Seng Hua, Petar Antov, and Puji Rahmawati Nurcahyani: resources and project administration; Widya Fatriasari, Apri Heri Iswanto, Harisyah Manurung: investigation; Muhammad Adly Rahandi Lubis, Mohd. Hazwan Hussin, Deded Sarip Nawawi: visualization, and investigation. All authors reviewed the results and approved the final version of the manuscript.

Availability of Data and Materials: Data are contained within the article.

Conflicts of Interest: The authors declare the following financial interests/personal relationships, which may be considered potential competing interests: Apri Heri Iswanto reports financial support provided by Universitas Sumatera Utara. Financial support (materials) for the Widya Fatriasari reports was provided

by PT Greenei Alam Indonesia (PT GAI). The other authors declare that they have no known competing financial interests or personal relationships that could have appeared to influence the work reported in this paper.

References

1. ImarchGroup. Particle board market: global industry trends, share, size, growth, opportunity and forecast 2023–2028. ImarcGroup; 2024.
2. Wibowo ES, Lubis MAR, Park BD. *In-situ* modification of low molar ratio urea-formaldehyde resins with cellulose nanofibrils for plywood. J Adhes Sci Technol. 2021;35(22):2452–65. doi:10.1080/01694243.2021.1890370.
3. Dazmiri M, Kiamahalleh M, Valizadeh Kiamahalleh M, Mansouri HR, Moazami V. Revealing the impacts of recycled urea-formaldehyde wastes on the physical-mechanical properties of MDF. Eur J Wood Wood Prod. 2019;77:293–9. doi:10.1007/s00107-018-1375-z.
4. Park BD, Ayrilmis N, Kwon JH, Han TH. Effect of microfibrillated cellulose addition on thermal properties of three grades of urea-formaldehyde resin. Int J Adhes Adhes. 2017;72:75–9. doi:10.1016/j.ijadhadh.2016.10.003.
5. Costa NA, Pereira J, Ferra J, Cruz P, Martins J, Magalhães FD, et al. Scavengers for achieving zero formaldehyde emission of wood-based panels. Wood Sci Technol. 2013;47(6):1261–72. doi:10.1007/s00226-013-0573-4.
6. Kawalerczyk J, Walkiewicz J, Mirski R, Dziurka D. Hemp flour as a formaldehyde scavenger for melamine-urea-formaldehyde adhesive in plywood production. BioResources. 2020;15:4052–64. doi:10.15376/biores.
7. Hemmilä V, Adamopoulos S, Karlsson O, Kumar A. Development of sustainable bio-adhesives for engineered wood panels—a review. RSC Adv. 2017;7(61):38604–30. doi:10.1039/C7RA06598A.
8. Siahkamari M, Emmanuel S, Hodge DB, Nejad M. Lignin-glyoxal: a fully biobased formaldehyde-free wood adhesive for interior engineered wood products. ACS Sustain Chem Eng. 2022;10(11):3430–41. doi:10.1021/acssuschemeng.1c06843.
9. Umemura K, Sugihara O, Kawai S. Investigation of a new natural adhesive composed of citric acid and sucrose for particleboard. J Wood Sci. 2013;59(3):203–8. doi:10.1007/s10086-013-1326-6.
10. Umemura K, Ueda T, Munawar S, Kawai S. Application of citric acid as natural adhesive for wood. J Appl Polym Sci. 2012;123:1991–6. doi:10.1002/app.v123.4.
11. Sun S, Zhao Z, Umemura K. Further exploration of sucrose-citric acid adhesive: synthesis and application on plywood. Polymers. 2019;11(11):1875. doi:10.3390/polym11111875.
12. Umemura K, Sugihara O, Kawai S. Investigation of a new natural adhesive composed of citric acid and sucrose for particleboard II: effects of board density and pressing temperature. J Wood Sci. 2014;61:40–4.
13. Widyorini R, Nugraha P, Rahman M, Prayitno T. Bonding ability of a new adhesive composed of citric acid-sucrose for particleboard. BioResources. 2016;11:4526–35.
14. Arias A, González-Rodríguez S, Vetroni Barros M, Salvador R, de Francisco AC, Moro Piekarski C, et al. Recent developments in bio-based adhesives from renewable natural resources. J Clean Prod. 2021;314:127892. doi:10.1016/j.jclepro.2021.127892.
15. Soubam T, Gupta A. Eco-friendly natural rubber latex and modified starch-based adhesive for wood-based panels application—a review. MIJEEC. 2021;3:49–53.
16. Valenzuela J, Leyser Ev, Pizzi A, Westermeyer C, Gorrini B. Industrial production of pine tannin-bonded particleboard and MDF. Holz als Roh-und Werkstoff. 2012;5(70):735–40.
17. Zhou XJ, Du GB. Applications of tannin resin adhesives in the wood industry. In: Alfredos A, editor. Applications of tannin resin adhesives in the wood industry. UK: IntechOpen; 2019.
18. Neitzel N, Hosseinpourpia R, Walther T, Adamopoulos S. Alternative materials from agro-industry for wood panel manufacturing—a review. Materials. 2022;15(13):4542. doi:10.3390/ma15134542.
19. Emmanuel Miassi Y, Fabrice Dossa K. Circular economy initiatives for forest-based bioeconomy: harnessing the potential of non-wood biomaterials. Waste Manage Bul. 2024;2(2):270–8. doi:10.1016/j.wmb.2024.05.006.

20. Kalita P, Dixit U, Mahanta P, Saha U. A novel energy efficient machine for plate manufacturing from areca palm leaf sheath. J Sci Ind Res. 2008;67:807–11.
21. Chen C, Sun G, Chen G, Li X, Wang G. Microscopic structural features and properties of single fibers from different morphological parts of the windmill palm. BioResources. 2017;12(2):3504–20.
22. Hertati L, Puspitawati L, Gantino R, Ilyas M. The meaning of creative industry, local wisdom, waste crafts, areca leaf sheath communities, mendis village suburban communities. Indonesia Berdaya. 2021;2:103–1 (In Indonesia).
23. Putri M, Faryuni I, Nurhasanah N. Fabrication of composite boards based on areca fiber (*Areca catechu* L.) and coconut fiber (*Cocos nucifer*a L.). Prisma Fisika. 2020;7:223 (In Indonesia).
24. Madyaratri EW, Ridho MR, Iswanto AH, Osvaldová LM, Lee SH, Antov P, et al. Effect of lignin or lignosulfonate addition on the fire resistance of areca (*Areca catechu*) particleboards bonded with ultra-low-emitting urea-formaldehyde resin. Fire. 2023;6(8):299. doi:10.3390/fire6080299.
25. Margarida Martins M, Carvalheiro F, Gírio F. An overview of lignin pathways of valorization: from isolation to refining and conversion into value-added products. Biomass Convers. 2024;14(3):3183–207. doi:10.1007/s13399-022-02701-z.
26. Statista. Statista production of paper and paperboard worldwide from 1961 to 2022, by major country (in million metric tons). Available from: https://www.statista.com/studies-and-reports/. [Accessed 2022].
27. Madyaratri EW, Iswanto AH, Nawawi DS, Lee SH, Fatriasari W. Improvement of thermal behavior of rattan by lignosulphonate impregnation treatment. Forests. 2022;13(11):1773. doi:10.3390/f13111773.
28. Neeraj M, Aurélie C, François R, Stéphane G, Fabine S, Giulio M, et al. An overview on the use of lignin and its derivatives in fire retardant polymer systems. In: Matheuss P, editor. An overview on the use of lignin and its derivatives in fire retardant polymer systems. UK: IntechOpen; 2018.
29. Laoutid F, Vahabi H, Saeb MR, Dubois P. Chapter 6—Lignin as a flame retardant for biopolymers. In: Puglia D, Santulli C, Sarasinis F, editors. Netherlands: Elsevier; 2022.
30. Liu W, Chen DQ, Wang YZ, Wang DY, Qu MH. Char-forming mechanism of a novel polymeric flame retardant with char agent. Polym Degrad Stab. 2007;92(6):1046–52. doi:10.1016/j.polymdegradstab.2007.02.009.
31. Lawson J, Srivastava D. Formation and structure of amorphous carbon char from polymer materials. Phys Rev B. 2008;77:144209. doi:10.1103/PhysRevB.77.144209.
32. Sinha Ray S, Kuruma M. Melt-dripping and char formation. In: Sinha Ray S, Kurumas M, editors. Melt-dripping and char formation. Gewerbestrasse, Cham, Switzerland: Springer; 2020.
33. Huang C, He J, Liang C, Tang S, Yong Q. Progress in applications of high value-added lignin materials. J For Eng. 2019;4(1):17–26.
34. Lizundia E, Sipponen MH, Greca LG, Balakshin M, Tardy BL, Rojas OJ, et al. Multifunctional lignin-based nanocomposites and nanohybrids. Green Chem. 2021;23(18):6698–760. doi:10.1039/D1GC01684A.
35. Prieur B, Meub M, Wittemann M, Klein R, Bellayer S, Fontaine G, et al. Phosphorylation of lignin: characterization and investigation of the thermal decomposition. RSC Adv. 2017;7:16866–77. doi:10.1039/C7RA00295E.
36. Maitz S, Schlemmer W, Hobisch MA, Hobisch J, Kienberger M. Preparation and characterization of a water-soluble kraft lignin. Adv Sustain Syst. 2020;4(8):2000052. doi:10.1002/adsu.v4.8.
37. Chrobak J, Iłowska J, Chrobok A. Formaldehyde-free resins for the wood-based panel industry: alternatives to formaldehyde and novel hardeners. Molecules. 2022;27(15):4862. doi:10.3390/molecules27154862.
38. Marturano V, Marotta A, Agustin-Salazar S, Ambrogi V, Cerruti P. Recent advances in bio-based functional additives for polymers. Prog Mater Sci. 2023;139(6):101186. doi:10.1016/j.pmatsci.2023.101186.
39. Costes L, Laoutid F, Aguedo M, Richel A, Brohez S, Delvosalle C, et al. Phosphorus and nitrogen derivatization as efficient route for improvement of lignin flame retardant action in PLA. Eur Polym J. 2016;84:652–67. doi:10.1016/j.eurpolymj.2016.10.003.
40. Ridho MR, Lubis MAR, Nawawi DS, Fatriasari W. Optimization of areca leaf sheath nanolignin synthesis by a mechanical method for *in situ* modification of ultra-low molar ratio urea-formaldehyde adhesives. Int J Biol Macromol. 2024;271:132614. doi:10.1016/j.ijbiomac.2024.132614.

41. Fitrianum F, Lubis MAR, Hadi YS, Sari RK, Maulana MI, Kristak L, et al. Adhesion and cohesion strength of phenol-formaldehyde resin mixed with different types and levels of catalyst for wood composites. J Compos Sci. 2023;7(8):310. doi:10.3390/jcs7080310.
42. Renzy Hariz T, Hadi Y, Lubis MA, Maulana M, Sari R, Hidayat W. Physical and mechanical properties of cross-laminated timber made of a combination of mangium-puspa wood and polyurethane adhesive. J Sylva Lestari. 2023;11:37–65. doi:10.23960/jsl.v11i1.
43. JSA. JIS A 5908:2003. Particleboards. Tokyo: Japanese Standards Association; 2003.
44. BSN. How to burn building materials for fire hazard prevention in houses and buildings. Jakarta: Badan Standarisasi Nasional; 2008 (In Indonesia).
45. Dillard DA. Physical properties of adhesives. In: da Silva LFM, Öchsner A, Adamss RD, editors. Physical properties of adhesives. Berlin, Heidelberg: Springer; 2011.
46. Sanghvi MR, Tambare OH, More AP. Performance of various fillers in adhesives applications: a review. Polym Bull. 2022;79(12):10491–553. doi:10.1007/s00289-021-04022-z.
47. BSN. SNI 06-0060-1987: about liquid formaldehyde phenol adhesives for plywood. Jakarta: BSN; 1987 (In Indonesia).
48. Shi SQ, Gardner DJ. Dynamic adhesive wettability of wood. Wood Fiber Sci. 2001;33(1):58–68.
49. Park BD, Kang EC, Park JY. Differential scanning calorimetry of urea-formaldehyde adhesive resins, synthesized under different pH conditions. J Appl Polym Sci. 2006;100(1):422–7. doi:10.1002/app.v100:1.
50. Tian H, Zhang Q, Pizzi A, Lei H, Wang J, Xi X. Adhesion properties and formaldehyde emissions of MnO_2/UF nanocomposite adhesives. Int J Adhes Adhes. 2024;128:103527. doi:10.1016/j.ijadhadh.2023.103527.
51. Wibowo ES, Kusumah SS, Subyakto, Umemura K. Modification of novel bio-based adhesive made from citric acid and sucrose by $ZnCl_2$. Int J Adhes Adhes. 2021;108:102866. doi:10.1016/j.ijadhadh.2021.102866.
52. Lima Natarelli CV, Lemos A, Assis M, Tonoli GHD, Trugilho P, Marconcini JM, et al. Sulfonated kraft lignin addition in urea-formaldehyde resin: thermokinetic analysis. J Therm Anal Calorim. 2019;137:1537–47. doi:10.1007/s10973-019-08075-1.
53. Younesi-Kordkheili H, Pizzi A. Lignin-based wood adhesives: a comparison between the influence of soda and Kraft lignin. Int J Adhes Adhes. 2023;121:103312. doi:10.1016/j.ijadhadh.2022.103312.
54. He X, Luzi FD, Yang W, Xiao Z, Torre L, Xie Y, et al. Citric acid as green modifier for tuned hydrophilicity of surface modified cellulose and lignin nanoparticles. ACS Sustain Chem Eng. 2018;6(8):9966–78. doi:10.1021/acssuschemeng.8b01202.
55. Ramadhoni B, Rahayu T, Rifathin A, Radini FA, Ichsan MZN, Mujadid A, et al. Improved thermal properties of lignin via phosphorylation using disodium hydrogen phosphate dodecahydrate salt. AIP Conf Proc. 2023;2902(1):050005.
56. Prieur B, Meub M, Wittemann M, Klein R, Bellayer S, Fontaine G, et al. Phosphorylation of lignin to flame retard acrylonitrile butadiene styrene (ABS). Polym Degrad Stab. 2016;127:32–43. doi:10.1016/j.polymdegradstab.2016.01.015.
57. Rusmirović J, Daničić D, Kovačević T, BogosavljeviĆ M, BrziĆ S, MarinkoviĆ A, et al. Phosphorylated kraft lignin based flame retardant: Efficient method for improvement of lignin flame retardancy and mechanical action in polyester. In: 8th International Scientific Conference of Defensive Technologies; 2018; Belgrade, Serbia. p. 538–43.
58. Li C, Lei H, Wu Z, Xi X, Du G, Pizzi A. Fully biobased adhesive from glucose and citric acid for plywood with high performance. ACS Appl Mater Interfaces. 2022;14(20):23859–67. doi:10.1021/acsami.2c02859.
59. Qian Y, Zuo C, Tan J, He J. Structural analysis of bio-oils from sub-and supercritical water liquefaction of woody biomass. Energy. 2007;32(3):196–202. doi:10.1016/j.energy.2006.03.027.
60. Myglovets M, Poddubnaya OI, Sevastyanova O, Lindström ME, Gawdzik B, Sobiesiak M, et al. Preparation of carbon adsorbents from lignosulfonate by phosphoric acid activation for the adsorption of metal ions. Carbon. 2014;80(1):771–83.

61. Ong HR, Prasad R, Khan M, Kabir Chowdhury MN. Effect of Palm kernel meal as melamine urea formaldehyde adhesive extender for plywood application: using a fourier transform infrared spectroscopy (FTIR) study. Appl Mech Mater. 2011;121–126:493–8.
62. Li C, Zhang J, Yi Z, Yang H, Zhao B, Zhang W, et al. Preparation and characterization of a novel environmentally friendly phenol-formaldehyde adhesive modified with tannin and urea. Int J Adhes Adhes. 2016;66:26–32. doi:10.1016/j.ijadhadh.2015.12.004.
63. Poljanšek I, Šebenik U, Krajnc M. Characterization of phenol-urea–formaldehyde resin by inline FTIR spectroscopy. J Appl Polym Sci. 2006;99(5):2016–28. doi:10.1002/app.22161.
64. Aizat AG, Paiman B, Lee SH, Zaidon A. Physico-mechanical properties and formaldehyde emission of rubberwood particleboard made with UF resin admixed with ammonium and aluminium-based hardeners. Pertanika J Sci Technol. 2019;27(1):473–88.
65. Jada SSJ. The structure of urea—formaldehyde resins. J Appl Polym Sci. 1988;35(6):1573–92. doi:10.1002/app.1988.070350614.
66. Park BD, Kim YS, Singh AP, Lim KPJ. Reactivity, chemical structure, and molecular mobility of urea-formaldehyde adhesives synthesized under different conditions using FTIR and solid-state 13C CP/MAS NMR spectroscopy. J Appl Polym Sci. 2003;88(11):2677–87. doi:10.1002/app.12115.
67. Li J, Zhang Y. Morphology and crystallinity of urea-formaldehyde resin adhesives with different molar ratios. Polymers. 2021;13(5):673. doi:10.3390/polym13050673.
68. Myers GE. Investigation of urea-formaldehyde polymer cure by infrared. J Appl Polym Sci. 1981;26(3):747–64. doi:10.1002/app.07.v26:3.
69. Younesi-Kordkheili H, Kazemi S, Behrooz R, Pizzi AP. Improving urea formaldehyde resin properties by glyoxalated soda bagasse lignin. Eur J Wood Wood Prod. 2014;73:77–85.
70. Boussetta A, Benhamou AA, Barba FJ, Idrissi MEL, Grimi N, Moubarik A. Experimental and theoretical investigations of lignin-urea-formaldehyde wood adhesive: density functional theory analysis. Int J Adhes Adhes. 2021;104:102737. doi:10.1016/j.ijadhadh.2020.102737.
71. Nuryawan A, Rahmawaty, Tambun KDS, Risnasari I, Masruchin N. Hydrolysis of particleboard bonded with urea-formaldehyde resin for recycling. Heliyon. 2020;6(5):e03936. doi:10.1016/j.heliyon.2020.e03936.
72. Del Menezzi C, Amirou S, Pizzi A, Xi X, Delmotte L. Reactions with wood carbohydrates and lignin of citric acid as a bond promoter of wood veneer panels. Polymers. 2018;10(8):833. doi:10.3390/polym10080833.
73. Umemura K, Kawai S. Development of wood-based materials bonded with citric acid. For Prod J. 2015;65(1–2):38–42.
74. Perez Locas C, Yaylayan VA. Isotope labeling studies on the formation of 5-(hydroxymethyl)-2-furaldehyde (HMF) from sucrose by pyrolysis-GC/MS. J Agric Food Chem. 2008;56(15):6717–23. doi:10.1021/jf8010245.
75. Li D, Yu L, Li L, Liang J, Wu Z, Xu X, et al. Melamine–urea–formaldehyde resin adhesive modified with recycling lignin: preparation, structures and properties. Forests. 2023;14(8):1625. doi:10.3390/f14081625.
76. Hidayat W, Aprilliana N, Asmara S, Bakri S, Hidayati S, Banuwa IS, et al. Performance of eco-friendly particleboard from agro-industrial residues bonded with formaldehyde-free natural rubber latex adhesive for interior applications. Polym Compos. 2022;43(4):2222–33. doi:10.1002/pc.v43.4.
77. Poddar P, Asadulah Asad M, Saiful Islam M, Sultana S, Parvin Nur H, Chowdhury AMS. Mechanical and morphological study of arecanut leaf sheath (ALS), coconut leaf sheath (CLS) and coconut stem fiber (CSF). Sci Adv Mater. 2016;1(2):1–4.
78. Park S, Baker JO, Himmel ME, Parilla PA, Johnson DK. Cellulose crystallinity index: measurement techniques and their impact on interpreting cellulase performance. Biotechnol Biofuels. 2010;3:1–10.
79. Martínez AJJD, Jaramillo N, Álvarez-López C, Vásquez Á, Quintana G. Effect of the addition of lignin on the physical-mechanical properties of particleboards made with pine/hydrangea stems. Int Wood Prod J. 2022;13(1):15–20. doi:10.1080/20426445.2021.1998301.
80. Liao R, Xu J, Umemura K. Low density sugarcane bagasse particleboard bonded with citric acid and sucrose: effect of board density and additive content. BioResources. 2016;11(1):2174–85.

81. Wibowo ES, Park BD. Chemical and thermal characteristics of ion-exchanged lignosulfonate. Molecules. 2023;28(6):2755. doi:10.3390/molecules28062755.
82. Xu C, Ferdosian F. Utilization of Lignosulfonate as dispersants or surfactants, utilization of lignosulfonate as dispersants or surfactants. Berlin, Heidelberg: Springer; 2017. doi:10.1007/978-3-662-54959-9_5.
83. Lee SH, Md Tahir P, Lum WC, Tan LP, Bawon P, Park BD, et al. A review on citric acid as green modifying agent and binder for wood. Polymers. 2020;12(8):1692. doi:10.3390/polym12081692.
84. Frihart CR, Chaffee TL, Wescott JM. Long-term formaldehyde emission potential from UF- and NAF-Bonded particleboards. Polymers. 2020;12(8):1852. doi:10.3390/polym12081852.
85. Rozman HD, Tan KW, Kumar RN, Abubakar A, Mohd. Ishak ZA, Ismail H. The effect of lignin as a compatibilizer on the physical properties of coconut fiber-polypropylene composites. Eur Polym J. 2000;36(7):1483–94. doi:10.1016/S0014-3057(99)00200-1.
86. Eom YG, Kim HJ, Kim JS, Kim SM, Kim JA. Reduction of formaldehyde emission from particleboardsby bio-scavengers. J Korean Wood Sci Technol. 2006;34(5):29–41.
87. Wang Z, Xue J, Qu J, Liu W. Synthesis of wood lignin-urea-formaldehyde resin adhesive. Adv Mat Res. 2012;560–561:242–6.
88. Schäfer M, Roffael E. On the formaldehyde release of wood. Holz als Roh-und Werkstoff. 2000;58:259–64. doi:10.1007/s001070050422.
89. Salem M, Böhm M. Understanding of formaldehyde emissions from solid wood: an overview. BioResources. 2013;8:4775–90.
90. Weigl-Kuska M, Wimmer R, Sykacek E, Steinwender M. Wood-borne formaldehyde varying with species, wood grade, and cambial age. For Prod J. 2009;59:88–92.
91. Torero JL, Gerhard JI, Martins MF, Zanoni MAB, Rashwan TL, Brown JK. Processes defining smouldering combustion: integrated review and synthesis. Prog Energ Combust. 2020;81:100869. doi:10.1016/j.pecs.2020.100869.
92. Rein G. Smoldering combustion. In: Hurley MJ, Gottuk D, Hall JR, Harada K, Kuligowski E, Puchovsky J, et al., editors. Smoldering combustion. New York: Springer; 2016.
93. Ardebili H, Zhang J, Pecht MG. Qualification and quality assurance. In: Ardebili H, Zhang J, Pechts MG, editors. Encapsulation technologies for electronic applications. New York: William Andrew Publishing; 2019.